Benchmarking Second Order Methods for the Calculation of Vertical Electronic Excitation Energies: Valence and Rydberg States in Polycyclic Aromatic Hydrocarbons

ARTICLE *in* THE JOURNAL OF PHYSICAL CHEMISTRY A · SEPTEMBER 2009

Impact Factor: 2.69 · DOI: 10.1021/jp9037123 · Source: PubMed

5 AUTHORS, INCLUDING:

Keld Lars Bak
Aarhus University
52 PUBLICATIONS **2,295** CITATIONS
SEE PROFILE

Sten Rettrup
University of Copenhagen
51 PUBLICATIONS **530** CITATIONS
SEE PROFILE

Stephan P. A. Sauer
University of Copenhagen
179 PUBLICATIONS **3,566** CITATIONS
SEE PROFILE

Benchmarking Second Order Methods for the Calculation of Vertical Electronic Excitation Energies: Valence and Rydberg States in Polycyclic Aromatic Hydrocarbons†

Heidi H. Falden,† Kasper R. Falster-Hansen,† Keld L. Bak,‡ Sten Rettrup,† and Stephan P. A. Sauer*,†

Department of Chemistry, University of Copenhagen, Universitetsparken 5, DK-2100, Copenhagen Ø, Denmark, and Ingeniørhøjskolen i Århus, Dalgas Avenue 2, 8000 Århus C, Denmark

Received: April 22, 2009; Revised Manuscript Received: September 16, 2009

The performance of the six second order linear response methods RPA(D), SOPPA, SOPPA(CCSD), CIS(D), CC2, and CCSD, which include either noniterative or iterative doubles contributions, has been studied in calculations of vertical excitation energies. The benchmark set consisted of 39 valence and 76 Rydberg states of benzene and five polycyclic aromatic hydrocarbons. As reference values we have used the results of the corresponding calculations with the third order method CCSDR(3), which includes noniterative triples contributions. In addition we have also carried out equivalent calculations at the level of the random phase approximation as well as with the configuration interaction singles and multireference configuration interaction singles and doubles methods.

Introduction

Vertical electronic excitation energies can elegantly and conveniently be calculated with linear response or polarization propagator and equation of motion methods.[1−4] Several correlated response theory methods have been developed over the last 30 years based on multiconfigurational self-consistent field (MCSCF),[5,6] Møller−Plesset perturbation theory (MP),[7−17] and coupled cluster (CC) wave functions[14−46]

Among the most accurate methods are the CC based methods[45,47−49] including iterative triple or higher excitations such as, e.g., EOM-CCSDT[31,41,50] or CC3,[27,28,31] which is an approximation to the latter, or several methods which include noniterative triples corrections,[51−66] e.g., CCSDR(3).[55,56] Methods including triple excitations are, however, very expensive, as they scale formally as N^7 with the number of orbitals N. They are certainly not suitable yet for routine applications on medium size organic molecules.

Second order linear response methods, where the single electron excitation contribution is evaluated through second order in the fluctuation potential and the two-electron contributions are evaluated to lower order, are on the other hand applicable to much larger molecules. Several such approaches have been presented, which differ mainly in how the contributions of the two-electron excitations are treated. Although we are not dealing here with excitations which are dominated by two-electron excitations, the indirect contributions of these terms to the one-electron excitations are important and determine partially the performance of the second order methods. Some approaches are based on coupled cluster theory, such as CCSD,[18,21−24,30] where the double replacement dominated excitations are correct through first order and which scales as N^6, or an approximation to it called CC2,[26,29] where the double replacement dominated excitations are only correct through zeroth order and which scales as N^5. With the implementation of analytical gradients and the fast resolution of the identity approximation,[67−70] CC2 has become an important tool in the study of photochemical reactions.

Alternatively methods based on MP directly have been presented such as the second order polarization propagator approximation (SOPPA),[7,8,10,12,13] where the double replacement dominated excitations are again only correct through zeroth order and thus scales also as N^5 or SOPPA(CCSD)[14−16] which still has the same order of the excitations but employs coupled cluster singles and doubles amplitudes instead of the MP correlation coefficients. In the propagator calculation SOPPA-(CCSD) scales thus as N^5, but the generation of the CCSD amplitudes scales still as N^6. For linear response properties such as frequency dependent polarizabilities,[16,17,71,72] oscillator strength sum rules,[73−75] rotational g-factors,[76−79] and in particular indirect nuclear spin−spin coupling constants,[80−83] this leads to a significant improvement over SOPPA, whereas for shieldings[84] a similar effect is not always observed. Excitation energies, on the other hand, have not been studied yet with SOPPA(CCSD).

More approximate and computationally less demanding are methods which contain noniterative doubles corrections such as CIS(D)[70,85] or RPA(D)[9,11] which can be derived as approximations to CC2 or SOPPA by applying perturbation theory to the response theory eigenvalue problem of CC2 and SOPPA using CCS or RPA as the zeroth order solutions. This is the same approach as it is employed in the derivation of CCSDR(3) from CC3.

Based on a completely different idea are traditional configuration interaction methods (CI), where excitation energies are obtained as the difference between two explicitly calculated states, i.e., eigenvalues of the CI matrix. The simplest approach beyond taking orbital energy differences as qualitative approximation for excitation energies is CIS.[86] Going beyond this by inclusion of doubles leads to CISD, which however is notouriously unbalanced in the calculation of excitation energies as long as it is based on a single Hartree−Fock reference. Improvements require a multireference approach like MR-CISD,[87−89] which, however, becomes quickly too large as long as the whole space of virtual orbitals is included. The way out

† Part of the "Walter Thiel Festschrift".

* To whom correspondence should be addressed. E-mail: sauer@kiku.dk.
† University of Copenhagen.
‡ Ingeniørhøjskolen i Århus.

10.1021/jp9037123 CCC: $40.75
Published on Web 09/25/2009

of this dilemma is to employ improved virtual orbitals[90−92] and afterward to truncate the virtual space.

CC-based as well as MP-based second order linear response methods have been employed in calculation of excitation energies for small benchmark molecules[9,16,26,31,33,35,41−43,54−56,70,93−102] as well on larger organic molecules.[8,10,11,102−104,104,105,105−112] Furthermore Thiel and co-workers[113−115] have recently investigated the performance of the CC-based methods, CC2, CCSD, CCSDR(3), and CC3, in comparison with each other as well as with CASPT2 and three DFT approaches for a large set of organic chromophores. However, no systematic comparison of both MP and CC based linear response methods for larger molecules has to our knowledge been published so far.

The goal of this study is therefore to answer the following questions:

(1) Does CC2 reproduce on average the CCSDR(3) results more closely than CCSD as was seen in the previous studies by Thiel and co-workers?[113,115]

(2) How do the MP based linear response methods perform in the calculation of vertical excitation energies compared to comparable CC based linear response methods using CCSDR(3) as reference?

(3) How do the two SOPPA variants, RPA(D) and SOPPA(CCSD), perform compared to the "parent" method SOPPA?

(4) How does RPA(D) perform compared to CIS(D)?

As benchmark set we have chosen 39 valence and 76 Rydberg states singlet excitation energies in polycyclic aromatic hydrocarbons (PAH). PAHs constitute a large class of conjugated π-electron systems that are key molecular species in many branches of chemistry, such as interstellar, combustion, environmental, and materials science.[116−118] PAHs are detected, e.g., in meteorites, in which they are strong candidates for the carriers of interstellar infrared absorption bands.[117] From this group we have selected naphthalene, anthracene, phenanthrene, azulene, biphenylene, and the parent molecule benzene. The molecules in this section were selected for their benchmark ability, since they have been extensively studied by chemists, physicists, environmental chemists, and so on. A wide range of both experimental data and computational results have been published. Previous calculations on the same systems include SOPPA calculations on benzene, naphthalene, and anthracene[8,10] and CC2, CCSD, CCSDR(3), and CC3 calculations on benzene[106,119] with identical basis sets and geometries as well as CASSCF or CASPT2 studies,[120−124] a MRMP study[125] and a recent DFT/MRCI study.[126] Thus the current study presents also the first coupled cluster results including triples corrections for the vertical excitation energies of naphthalene, anthracene, phenanthrene, azulene, and biphenylene.

Details of the Calculations. Vertical excitation energies were calculated at the RPA, RPA(D), SOPPA, SOPPA(CCSD), CIS, CIS(D), CC2, CCSD, and CCSDR(3) levels of theory. For benzene and naphthalene we have also carried out MR-CISD calculations with modified virtual orbitals. In all calculations the frozen core approximation was employed, which in our previous study[10] was shown to have no significant effect on the vertical excitation energies.

All calculations were carried out with a local development version of the DALTON 2.0 code,[127] which includes the atomic integral direct implementation of the SOPPA, SOPPA(CCSD) and RPA(D) method,[9,10] and of the PEDICI program[128−131] which is interfaced to Dalton.

Geometries. With the exception of benzene we have employed optimized geometries from the literature. They were primarily taken from the work of Martin et al.,[116] who had optimized the geometries of naphthalene (cc-pVTZ), anthracene (cc-pVDZ), phenanthrene (cc-pVDZ), and azulene (cc-pVTZ) employing density functional theory (DFT) with the B3LYP functional and the basis set included in the parentheses. The geometry of biphenylene, taken from the work of Beck et al.,[123] was also optimized at the DFT level with the B3LYP functional but with the 6-31G* basis set.

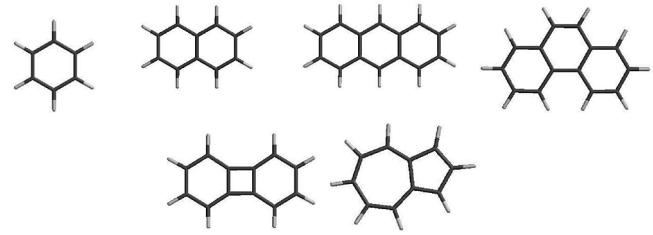

Figure 1. Structures of the studied PAHs: benzene, naphthalene, anthracene, phenanthrene (first row starting left), biphenylene, and azulene (second row starting left).

Benzene stands out from the rest with an extensive amount of literature and is clearly a very common benchmark molecule. The commonly employed geometry is almost the experimental geometry[132] obtained in X-ray studies as reported by Stevens et al.[133] Roos and co-workers[120,122] employed this geometry in their CASSCF and CASPT2 calculations and consequently also Packer et al.[8] in the first SOPPA calculation on benzene. We continue with this practice. Azulene is in a subgroup of the polycyclic aromatic hydrocarbons called nonalternant hydrocarbons due to the fact that it contains odd-membered rings. It is isoelectric to naphthalene, and although naphthalene is colorless and nonpolar, azulene is blue and has a large dipole moment. An early report of the structure and electronic spectrum of azulene by Pariser[134] suggested that azulene belongs to the C_{2v} symmetry group. But as discussed by Hinchliffe and Soscún[135] the structure of azulene in the gas-phase is unknown. At different levels of theory two possibilities emerge: a C_s and a C_{2v} structure with only a small difference between the two geometries. C_{2v} is more stable than C_s in the ground state. Murakami et al.[136] have calculated the in-plane asymmetric b_2 normal mode of the $1A_1$ and $1B_1$ states and concluded that the bond equalized C_{2v} structure yields a more stabilized structure than the bond-alternating C_s structure in the ground state. For the calculations in this work the C_{2v} geometry is therefore used. Phenanthrene like azulene has no center of symmetry. Possible resonance structures of phenanthrene have been discussed by Chakrabarti et al.[137] The classification of biphenylene has been intensively discussed.[123,138−142] Depending on how the electrons are counted, either as two benzene molecules with 6π electrons or collectively as 12π electrons, which equals $4n$ with $n = 3$, biphenylene should be considered as an aromatic or as an antiaromatic molecule. In the work of Beck et al.[123] it was argued that the length of the bonds between the two ring systems is large enough to ensure that there is no interaction between the two ring systems and that biphenylene can be regarded as an aromatic molecule. The experimentally observed ground state energy shows, that the bonds connecting the benzene molecules are indeed unusually long as reported by Fawcett et al.[143] The situation is completely different, however, for the first excited states, where the four membered ring changes drastically by going from a rectangular structure in the ground state to a square structure, as shown by Elsaesser et al.[139]

Basis Sets. We have employed the same basis sets as in the previous SOPPA studies on benzene, naphthalene, and anthra-

TABLE 1: Coefficients of the Diffuse Functions

molecule		s		p		d	
benzene	[1s1p1d]	0.024624	(0.4584)	0.042335	(0.0290)	0.060540	(0.0290)
		0.011253	(−2.0379)	0.019254	(−0.2025)	0.027446	(−0.2025)
		0.005858	(1.9778)	0.009988	(−0.2629)	0.014204	(−0.2629)
		0.003346	(−3.1952)	0.005689	(−0.4338)	0.008077	(−0.4338)
		0.002048	(3.7239)	0.003476	(0.0101)	0.004927	(0.0101)
		0.001324	(−3.1770)	0.002242	(−0.1587)	0.003175	(−0.1587)
		0.000893	(1.7028)	0.001511	(0.0831)	0.002137	(0.0831)
		0.000624	(−0.4214)	0.001055	(−0.0244)	0.001491	(−0.0244)
naphthalene	[2s2p2d]	0.009614		0.008778		0.006270	
azulene		0.003542		0.003234		0.002310	
anthracene	[3s3p3d]	0.010000		0.010000		0.010000	
biphenylene		0.003300		0.003300		0.003300	
phenanthrene		0.001100		0.001100		0.001100	

TABLE 2: Benzene: Vertical Singlet Excitation Energies (in eV) in Ascending Order of CCSDR(3) Energies

state		RPA	RPA(D)	SOPPA	SOPPA(CCSD)	CIS	CIS(D)	CC2	CCSD	CCSDR(3)	MR-CISD
					Valence $\pi\pi^*$						
$1B_{2u}$	($e_{1g} \rightarrow e_{2u}$)	5.82	4.82	4.69	4.52	6.03	5.31	5.27	5.19	5.12	5.77
$1B_{1u}$	($e_{1g} \rightarrow e_{2u}$)	5.88	6.36	6.01	5.92	6.19	6.68	6.56	6.59	6.56	6.73
$1E_{1u}$	($e_{1g} \rightarrow e_{2u}/3p_z$)	7.16	6.87	7.03	6.94	7.18	7.06	7.01	7.16	7.15	7.34
					Rydberg $\pi\pi^*$						
$1E_{2g}$	($e_{1g} \rightarrow (3d_{xz/yz})$)	7.80	7.54	7.54	7.48	7.80	7.66	7.64	7.84	7.85	7.98
$2A_{1g}$	($e_{1g} \rightarrow (3d_{xz/yz})$)	7.77	7.55	7.55	7.49	7.77	7.67	7.65	7.85	7.86	7.99
$1A_{2g}$	($e_{1g} \rightarrow (3d_{xz/yz})$)	7.85	7.57	7.58	7.52	7.85	7.68	7.67	7.87	7.88	8.00
					Rydberg $\pi\sigma^*$						
$1E_{1g}$	($e_{1g} \rightarrow 3s$)	6.55	6.20	6.17	6.12	6.55	6.38	6.33	6.47	6.45	6.68
$1A_{2u}$	($e_{1g} \rightarrow (3p_{x/y})$)	6.94	6.70	6.69	6.63	6.94	6.86	6.83	6.98	6.98	7.18
$1E_{2u}$	($e_{1g} \rightarrow (3p_{x/y})$)	7.11	6.76	6.75	6.69	7.12	6.91	6.88	7.05	7.04	7.25
$1A_{1u}$	($e_{1g} \rightarrow (3p_{x/y})$)	7.28	6.84	6.83	6.77	7.29	6.97	6.96	7.13	7.12	7.34
$1B_{1g}$	($e_{1g} \rightarrow 3d_{xy}$)	7.70	7.35	7.34	7.28	7.70	7.47	7.45	7.65	7.65	7.83
$1B_{2g}$	($e_{1g} \rightarrow 3d_{xy}$)	7.68	7.35	7.35	7.29	7.68	7.47	7.46	7.65	7.66	7.83

cene.[8,10] They are of the atomic natural orbital (ANO) type and consist of the C[4s3p1d]/H[2s1p], i.e., ANO1, basis set of Widmark et al.[144] However, in order to obtain a reasonable treatment of the Rydberg excitations diffuse functions must be added to these basis set. Due to the size of the Rydberg orbitals it is suffice to put the diffuse functions at the center of mass (CM) of the molecule. The extra diffuse functions consist of 8 even tempered s, p, and d sets of functions contracted to [1s1p1d] for benzene,[122] 2 sets of uncontracted s, p, and d functions (2s2p2d) for naphthalene[121] and 3 sets of uncontracted s, p, and d functions (3s3p3d) for anthracene.[10] The extra diffuse functions of naphthalene were also used in the calculations on azulene, and similarly the same diffuse functions were employed for biphenylene and phenanthrene as for anthracene. The coefficients of the diffuse functions are listed in Table 1 where the contraction coefficients are given in parentheses. Addition of more diffuse functions was previously shown[29,106,119] to change the results by less than 0.05 eV.

Results and Discussion

Vertical excitation energies have been calculated for benzene, naphthalene, anthracene, phenanthrene, azulene, and biphenylene using the RPA, RPA(D), SOPPA, SOPPA(CCSD), CIS, CIS(D), CC2, CCSD, and CCSDR(3) methods. In addition MR-CISD calculations were carried out for benzene and naphthalene using modified virtual orbitals. We use the CCSDR(3) results as reference, with which we compare the results of the second order methods, because CCSDR(3) was shown to reproduce almost quantitatively the results of CC3 calculations not only for small molecules[55,56,101] but also for benzene,[106] naphthalene[115] and other organic chromophores[102,107,108,110,115] with only a few but predictable exceptions. Experimental values[145−162] can be found for some of the states included in our study.

Benzene. The calculated results for the lowest 12 singlet excitation energies of benzene are listed in Table 2. The states are grouped according to their type of transitions, e.g. valence or Rydberg. Within a group they are given in the order of increasing CCSDR(3) excitation energy. Only the $n = 3$ Rydberg series, which converges to the first ionization potential of 9.25 eV, was included in our study. The assignment of the transitions follows that of Lorentzon et al.[122] They include two valence states, $1B_{2u}$ and $1B_{1u}$, one mixed valence and Rydberg state, $1E_{1u}$, and 9 dominant Rydberg states. The weight of the single excitations, % R_1, in the CCSD excitation energy calculations is 95% for all states apart from the $1B_{2u}$ state, where it is only 91%.

Considering the order of the calculated states first, we can see that the iterative second order methods, SOPPA, SOPPA(CCSD), CC2 and CCSD, as well as the noniterative methods, RPA(D) and CIS(D), and MR-CISD reproduce the order of the excited states as found in the CCSDR(3) calculations. However, one should note, that we only consider the lowest excited state in every irreducible representation. CIS and RPA, on the other hand, have problems reproducing the order of the $1E_{2g}$ and $2A_{1g}$ and of the $1B_{1g}$ and $1B_{2g}$ Rydberg states as given by CCSDR(3). Both pairs of transitions are predicted to be energetically very close by all second-order methods as well as by the reference CCSDR(3). Since CIS(D) and RPA(D) both reproduce the correct order of states, we have here the first example for the important effect of the noniterative doubles corrections in CIS(D) and RPA(D).

Comparing now the results of the different methods with the CCSDR(3) results we find that the deviations of the RPA results from the CCSDR(3) reference values depend extremely on the state under consideration. For the two valence states we find very large deviations +0.70 and −0.68 eV, for $1B_{2u}$ and $1B_{1u}$, and a very small one with only 0.01 eV for the mixed $1E_{1u}$ state, whereas the deviations for the Rydberg states range only between −0.09 and +0.16 eV. Inclusion of the second order and doubles corrections in RPA(D) changes this dramatically. The deviations from the CCSDR(3) reference values are thus in the range from −0.20 to −0.31 eV with the majority of energy differences between −0.28 and −0.31 eV. All of the RPA(D) energies are lower than the CCSDR(3) values. The smallest deviation is for the $1B_{1u}$ transition, whereas the largest deviations are found for the $1E_{2g}$, $2A_{1g}$, $1A_{2g}$, and $1B_{2g}$ states, i.e., for the transitions to the 3d Rydberg orbitals. This implies that the two valence states are in much better agreement with the reference values than at the RPA level but that the Rydberg states are actually in worse agreement. The SOPPA results are also all lower than the reference energies and the deviations are in the range from −0.12 to −0.55 eV. Most deviations are about −0.30 eV with three exceptions: the two valence transitions, $1B_{2u}$ and $1B_{1u}$, with −0.43 and −0.55 eV and the $1E_{1u}$ mixed transition with −0.12 eV. The deviations for the Rydberg transitions vary only between −0.28 and −0.31 eV. The deviations of the SOPPA(CCSD) results follow the SOPPA results with respect to which transitions are reproduced poorly. The range of deviations in the excitation energies is −0.21 to −0.64 eV again with the same three exceptions, the valence transitions: the $1B_{2u}$ transition with −0.60 eV, the $1B_{1u}$ transition with −0.64 eV, and the mixed $1E_{1u}$ transition with −0.21 eV. Taking these states aside the remaining differences from the reference results for the Rydberg transitions are in the range of −0.35 to −0.37 eV.

CIS, like RPA, does remarkably well for the Rydberg states and quite badly for the valence states included in our study. However, whereas the CIS results for the Rydberg states are indistinguishable from the RPA results, the valence states are predicted to be higher in energy. Similar to RPA(D), the addition of the second order and doubles corrections in CIS(D) leads to a much more uniform deviation from the CCSDR(3) results, although not as uniform as in the case of RPA(D). This implies an improved agreement with the CCSDR(3) results for the two valence states and a more uniform but in general worse agreement for the Rydberg transitions. On the other hand the CIS(D) results are all shifted to higher energies and thus in better agreement with the reference values than the RPA(D) results. The CC2 results underestimate the reference results for the Rydberg transitions by −0.21 to −0.12 eV which is in all cases slightly more than found in CIS(D). The situation is quite different for the valence states: the result for the $1B_{1u}$ state is in perfect agreement, whereas the $1B_{2u}$ is overestimated by 0.15 eV. Compared to SOPPA the CC2 results are all in better agreement with the CCSDR(3) results, as was already pointed out previously.[106] The CCSD results are very close to the reference values, as should be expected since the CCSDR(3) method adds only a correction to the calculated CCSD energies. The valence states are higher in energy than CCSDR(3) values with deviations in the range of 0.01−0.07 eV. Again a slightly poorer description of valence states is observed compared to the description of the Rydberg states.

The multireference space in the MR-CISD calculations is obtained by including all the configuration state functions (CSF's) generated by all single excitations from the highest occupied e_{1g} orbitals into the lowest 11 optimized virtual orbitals. It leads to 23 reference CSF's and a MR-CISD space formed by 28 935 182 spin adapted CSF's after truncating the total orbital space to 100 orbitals.

The MR-CISD results are a clear improvement over the CIS results for the two valence states but are in worse agreement for the Rydberg states than CIS. Compared with the other methods including double excitations, we can see that we obtain significantly higher excitation energies in our MR-CISD calculations. This applies to the Rydberg states and in particular to the lowest excited valence state.

Naphthalene. The calculated results for 21 singlet excited states of naphthalene are listed in Table 3. The states are again grouped according to their type of transitions, e.g., valence or Rydberg and are sorted according to increasing CCSDR(3) excitation energy. The assignment of the transitions follows that of Bak et al.[10] They include eight valence states, eleven Rydberg states and two states, $2B_{1g}$ and $4B_{2u}$, which in earlier calculations employing smaller basis sets[121,8] were assigned as valence transitions, but were later shown to exhibit significant Rydberg character.[10] The weight of the single excitations, % R_1, in the CCSD excitation energy calculations is 95% for all Rydberg states, whereas the valence states, and in particular the $1B_{3u}$ and $2A_g$ states with only 91%, have smaller weights.

Looking at the order of the states first again, we can see that RPA and CIS are less able to reproduce the order of the transitions as given by CCSDR(3) than in benzene. The two lowest states, $1B_{3u}$ and $1B_{2u}$, are interchanged, the energies of the $2A_g$ and $3B_{1g}$ states are predicted to be much too high and the order of the two pairs of states $2B_{2g}$ and $2B_{3g}$ and $3B_{2u}$ and $3B_{3u}$ are interchanged. Inclusion of the doubles contribution in RPA(D) and CIS(D) corrects some of these errors but not all. The two lowest valence states, e.g., have now the correct order, but the $2A_g$, $3A_g$, and $3B_{3u}$ states are now too low in energy. Furthermore the $2A_u$ and $2B_{1u}$ transitions as well as the $2B_{2u}$ and $3B_{1g}$ states and the $2B_{1g}$ and $3A_g$ transitions are now reversed by a few hundreds of an eV contrary to RPA and CIS. The iterative second order methods show the correct ordering with one exception, the $2A_g$ state relative to the $2B_{3u}$ state, which at the CCSDR(3) level is 0.19 eV higher in energy than $2A_g$, but has a lower energy at the SOPPA, SOPPA(CCSD) and even the CC2 level.

Comparing now the results of the different methods with the CCSDR(3) results we find that like for benzene the deviations of the RPA and CIS results for the valence states are partially very large and depend strongly on the state. The RPA energies are always smaller than the CIS energies and are in better agreement with the CCSDR(3) results with one exception. The range of deviations from the CCSDR(3) results is −0.26 to +1.14 eV for RPA and 0.04 to 1.23 eV for CIS. The agreement for the Rydberg transitions is better. The RPA and CIS results are identical and are scattered around the CCSDR(3) results with error bars of about ±0.2 eV, if we exclude the mixed valence−Rydberg $2B_{1g}$ state. This implies again that only the CCSD results are in better agreement with the CCSDR(3) results for the Rydberg states. Adding the second order doubles corrections in CIS(D) reduces the deviations significantly for all valence states but the $1B_{2u}$ state in CIS(D). RPA(D) on the other hand overestimates the corrections for three states, $1B_{1g}$, $2B_{3u}$, and $2B_{2u}$, which are now too low in energy. Nevertheless, the spread of deviations for the valence states is very similar in both methods, −0.80 to +0.03 eV for RPA(D) and −0.45 to +0.33 eV for CIS(D), with the CIS(D) results just being shifted to higher energies. For the Rydberg states we observe also again that the doubles corrections, destroys the good agreement with

TABLE 3: Naphthalene: Vertical Singlet Excitation Energies (in eV) in Ascending Order of CCSDR(3) Energies

state		RPA	RPA(D)	SOPPA	SOPPA(CCSD)	CIS	CIS(D)	CC2	CCSD	CCSDR(3)	MR-CISD
					Valence $\pi\pi^*$						
$1B_{3u}$	$(1a_u \rightarrow 4b_{3g})$	5.00	4.01	3.88	3.64	5.22	4.51	4.47	4.44	4.38	4.91
$1B_{2u}$	$(1a_u \rightarrow 4b_{2g})$	4.75	4.94	4.34	4.17	5.08	5.23	4.89	5.13	5.01	5.47
$1B_{1g}$	$(1a_u \rightarrow 5b_{1u})$	6.04	5.80	5.56	5.45	6.06	5.98	5.87	6.08	6.02	6.06
$2A_g$	$(2b_{1u} \rightarrow 5b_{1u})$ $(2b_{1u} \rightarrow 4b_{2g})$	7.22	6.11	5.65	5.48	7.31	6.41	6.18	6.21	6.08	6.73
$2B_{3u}$	$(1a_u \rightarrow 4b_{3g})$ $(2b_{1u} \rightarrow 4b_{2g})$	6.50	5.85	5.65	5.38	7.02	6.38	6.15	6.43	6.27	6.66
$2B_{2u}$	$(2b_{1u} \rightarrow 4b_{3g})$	6.73	5.99	5.97	5.74	7.21	6.40	6.47	6.66	6.51	6.68
$3B_{1g}$	$(1b_{3g} \rightarrow 4b_{2g})$	7.86	5.96	6.26	6.14	7.91	6.31	6.70	6.91	6.76	7.49
$4A_g$	$(1b_{2g} \rightarrow 4b_{2g})$	7.78	7.40	7.43	7.29	7.78	7.48	7.50	7.71	7.56	8.46
					Rydberg $\pi\pi^*$						
$1B_{2g}$	$(1a_u \rightarrow 3p_y)$	5.97	5.69	5.66	5.58	5.97	5.85	5.80	6.00	5.99	5.95
$1B_{3g}$	$(1a_u \rightarrow 3p_x)$	6.03	5.71	5.68	5.60	6.03	5.87	5.82	6.02	6.00	6.00
$2A_u$	$(1a_u \rightarrow 3d_{x^2-y^2})$	6.53	6.27	6.24	6.15	6.53	6.39	6.35	6.58	6.57	6.51
$2B_{1u}$	$(1a_u \rightarrow 3d_{xy})$	6.58	6.26	6.28	6.19	6.58	6.38	6.38	6.62	6.61	6.66
$2B_{2g}$	$(2b_{1u} \rightarrow 3p_x)$	6.81	6.39	6.36	6.23	6.82	6.54	6.50	6.67	6.67	6.72
$2B_{3g}$	$(2b_{1u} \rightarrow 3p_y)$	6.90	6.51	6.41	6.28	6.90	6.63	6.55	6.72	6.72	6.77
$3B_{2u}$	$(1a_u \rightarrow 3d_{xz})$	6.67	6.46	6.46	6.38	6.67	6.57	6.55	6.80	6.80	7.31
$3B_{3u}$	$(1a_u \rightarrow 3d_{yz})$	6.74	6.40	6.50	6.41	6.64	6.49	6.58	6.85	6.84	7.14
$4B_{2u}$	$(1a_u \rightarrow 4d_{xz})$	7.20	6.97	6.98	6.89	7.20	7.00	7.01	7.34	7.35	7.48
					Rydberg $\pi\sigma^*$						
$1A_u$	$(1a_u \rightarrow 3s)$	5.60	5.30	5.26	5.17	5.60	5.47	5.42	5.59	5.57	5.55
$1B_{1u}$	$(2b_{1u} \rightarrow 3s)$	6.39	6.02	5.96	5.83	6.39	6.19	6.12	6.25	6.24	6.29
$2B_{1g}$	$(1a_u \rightarrow 3p_z)$	6.56	6.37	5.97	5.86	6.75	6.66	6.25	6.58	6.39	6.90
$3A_g$	$(2b_{1u} \rightarrow 3p_z)$	6.87	6.34	6.61	6.48	6.89	6.60	6.76	6.90	6.91	7.02

the CCSDR(3) results by shifting the energies 0.2 to 0.4 eV (RPA(D)) or 0.1 to 0.3 eV (CIS(D)) toward lower energies. The CIS(D) pure Rydberg excitation energies are thus all higher than the RPA(D) ones, but also smaller than the CCSDR(3) values. In SOPPA all valence states but the $3B_{1g}$ and $4A_g$ states are lower in energy than in RPA(D) and thus in worse agreement with the CCSDR(3) reference values. However, the spread of deviations is slightly reduced to between −0.67 and −0.13 eV. Replacement of the Møller−Plesset correlation coefficients by CCSD amplitudes in SOPPA(CCSD) reduces the valence excitation energies even further and thus increases the deviations from the CCSDR(3) results. The same trend is also observed for the Rydberg states, where the SOPPA(CCSD) results are about 0.1 eV lower than the SOPPA results, which are for the majority of the states also lower than the RPA(D) results. However, the span of deviations is also reduced in the series RPA(D), SOPPA and SOPPA(CCSD) to only 0.06 eV in the latter method, meaning that SOPPA(CCSD) underestimates the CCSDR(3) results for the Rydberg states by 0.42 ± 0.03 eV.

The two coupled cluster methods, CC2 and CCSD, on the other hand, show the smallest deviations from the CCSDR(3) results for the valence states. CCSD always overestimates the CCDSR(3) results, whereas CC2 underestimates the majority of the CCSDR(3) results. For 6 out of the 8 valence states CC2 is in better agreement with the CCSDR(3) valence state values than CCSD. For the Rydberg states the situation is reversed. The CCSD results are basically indistinguishable from the CCSDR(3) values, whereas the CC2 results are for the majority of the Rydberg states in slightly worse agreement than the CIS(D) values.

The multireference space in the MR-CISD calculations is obtained by including all the configuration state functions (CSF's) generated by all single excitations from the highest occupied orbitals, $1b_{2g}$, $1b_{3g}$, $2b_{1u}$, and $1a_u$, into a the lowest 12 virtual orbitals. It leads to 49 reference CSF's and a MR-CISD space formed by 103 861 609 spin adapted CSF's. As in the benzene case the total orbital space is truncated to 100.

For the MR-CISD results we observe quite a different behavior than for benzene. First of all the MR-CISD results are not always higher than the CCSDR(3) results. Second, the MR-CISD results are only for three of the valence states, $1B_{3u}$, $2B_{3u}$, and $2B_{2u}$, a clear improvement over the CIS results. All the valence excitation energies are overestimated for the MR-CISD calculations compared with CCSDR(3). Generally, the Rydberg states are are in good agreement with the CCSDR(3) results apart from the states $3B_{2u}$, $3B_{3u}$, and $2B_{1g}$ where the excitation energies are overestimated by 0.51, 0.30, and 0.51 eV which is more than the CIS estimates.

Azulene. For azulene we have calculated excitation energies to 4 valence and 16 Rydberg states. The results are given in Table 4. The weight of the single excitations, % R_1, in the CCSD excitation energy calculations is ≈ 95% for all Rydberg states, whereas the valence states, and in particular the $1B_2$ and $2B_2$ states with only 91%, have smaller weights.

The $5A_1$ and $6A_1$ Rydberg states are almost degenerate at the CCSDR(3) level, the latter is less than 0.01 eV higher in energy. All other methods, however, underestimate the energy of the $6A_1$ Rydberg state slightly more than the energy of the $5A_1$ Rydberg state and predict therefore the wrong order of these two Rydberg states. Experimentally these two states are also very close as reported by Foggi et al.[162] RPA and CIS get also the order of the $3B_1$ and $4B_2$ Rydberg states wrong, which is corrected at the RPA(D) but not at the CIS(D) level. Furthermore CIS(D) predicts the $4A_1$ Rydberg state to be lower than the $4B_2$ state contrary to all other methods.

For the valence states we find again that the deviations of the RPA and CIS results from the CCSDR(3) reference results and from each other are are partially very large and depend strongly on the state. For three out of the four states, the RPA results are closer to the reference values than the CIS results. Adding the noniterative second order corrections in RPA(D) leads to large changes and improves the agreement with CCSDR(3) for two states. All RPA(D) excitation energies are also smaller than the reference values. In the iterative MP

TABLE 4: Azulene: Vertical Singlet Excitation Energies (in eV) in Ascending Order of CCSDR(3) Energies

	state	RPA	RPA(D)	SOPPA	SOPPA(CCSD)	CIS	CIS(D)	CC2	CCSD	CCSDR(3)
					Valence $\pi\pi^*$					
$1B_2$	$(2b_1 \rightarrow 8a_2)$	2.57	1.78	1.63	1.29	2.88	2.31	2.31	2.29	2.25
$2A_1$	$(2a_2 \rightarrow 5a_2)$	3.62	3.96	3.31	3.09	3.97	4.15	3.95	4.03	3.99
$2B_2$	$(3b_1 \rightarrow 5a_2)$	5.09	4.35	4.08	3.75	5.53	4.88	4.70	4.81	4.66
$3A_1$	$(2a_2 \rightarrow 5a_2)$	5.29	4.42	4.18	3.84	5.76	5.25	4.89	5.28	5.05
					Rydberg $\pi\pi^*$					
$1A_2$	$(2a_2 \rightarrow 3s)$	4.85	4.52	4.42	4.29	4.85	4.71	4.63	4.78	4.79
$3B_2$	$(2b_1 \rightarrow 3p_z)$	5.37	5.12	5.10	4.96	5.34	5.23	5.27	5.42	5.45
$3B_1$	$(3b_1 \rightarrow 3s)$	5.95	5.66	5.57	5.42	5.96	5.84	5.77	5.90	5.89
$4B_2$	$(2b_1 \rightarrow 3d_{yz})$	5.89	5.68	5.66	5.52	5.89	5.80	5.78	5.99	6.04
$4A_1$	$(2a_2 \rightarrow 3d_{xz})$	5.91	5.69	5.68	5.54	6.00	5.56	5.80	6.02	6.06
$5B_2$	$(2b_1 \rightarrow 4p_z)$	6.17	5.95	5.94	5.79	6.17	6.03	5.99	6.22	6.13
$5A_1$	$(3b_1 \rightarrow 3p_z)$	6.46	6.30	6.26	6.09	6.48	6.42	6.43	6.54	6.54
$6A_1$	$(2a_2 \rightarrow 4d_{xz})$	6.41	6.19	6.17	6.02	6.42	6.25	6.24	6.53	6.55
					Rydberg $\pi\sigma^*$					
$1B_1$	$(2a_2 \rightarrow 3p_x)$	5.22	4.91	4.85	4.71	5.22	5.07	5.03	5.19	5.22
$2A_2$	$(2a_2 \rightarrow 3p_y)$	5.30	4.96	4.92	4.78	5.30	5.12	5.09	5.25	5.28
$3A_2$	$(2a_2 \rightarrow 3d_{xx})$	5.76	5.51	5.44	5.31	5.76	5.64	5.59	5.78	5.82
$2B_1$	$(2a_2 \rightarrow 3d_{xy})$	5.76	5.51	5.48	5.34	5.76	5.64	5.61	5.81	5.85
$4A_2$	$(2a_2 \rightarrow 3d_{zz})$	5.80	5.55	5.54	5.40	5.80	5.67	5.68	5.86	5.91
$5A_2$	$(2a_2 \rightarrow 3d_{yy})$	6.00	5.78	5.75	5.61	6.00	5.88	5.86	6.09	6.15
$4B_1$	$(2a_2 \rightarrow 4p_x)$	6.14	5.90	5.88	5.74	6.14	5.99	5.98	6.23	6.29
$5B_1$	$(3b_1 \rightarrow 4p_y)$	6.33	6.05	6.02	5.87	6.33	6.21	6.19	6.33	6.34

TABLE 5: Anthracene: Vertical Singlet Excitation Energies (in eV) in Ascending Order of CCSDR(3) Energies

	state	RPA	RPA(D)	SOPPA	SOPPA(CCSD)	CIS	CIS(D)	CC2	CCSD	CCSDR(3)
					Valence $\pi\pi^*$					
$1B_{3u}$	$(2b_{2g} \rightarrow 6b_{1u})$	4.31	3.38	3.24	2.91	4.56	3.89	3.85	3.85	3.80
$1B_{2u}$	$(2b_{3g} \rightarrow 6b_{1u})$	3.68	3.68	3.08	2.83	4.04	3.96	3.66	4.00	3.85
$1B_{1g}$	$(1a_u \rightarrow 6b_{1u})$	6.73	4.81	4.63	4.48	6.75	5.13	5.10	5.57	5.25
$2B_{2u}$	$(2b_{3g} \rightarrow 5b_{1u})$	5.31	5.11	4.88	4.74	5.32	5.30	5.17	5.39	5.35
$2B_{1g}$	$(2b_{3g} \rightarrow 6b_{2g})$	5.42	5.10	4.70	4.52	5.69	5.52	5.27	5.53	5.39
$2A_g$	$(1a_u \rightarrow 2a_u)$	6.56	5.39	4.99	4.80	6.69	5.57	5.56	5.62	5.46
$2B_{3u}$	$(2b_{3g} \rightarrow 2a_u)$	5.80	4.94	4.82	4.47	6.20	5.41	5.36	5.69	5.52
					Rydberg $\pi\sigma^*$					
$1B_{3g}$	$(2b_{3g} \rightarrow 3s)$	4.94	4.69	4.52	4.52	4.94	4.88	4.81	4.99	4.98
$1B_{1u}$	$(2b_{3g} \rightarrow 3p_y)$	5.22	4.98	4.95	4.82	5.23	5.15	5.09	5.30	5.29
$1A_u$	$(2b_{3g} \rightarrow 3p_x)$	5.33	5.06	5.01	4.89	5.33	5.22	5.15	5.37	5.35
$2B_{3g}$	$(2b_{3g} \rightarrow 3d_{x^2-y^2})$	5.68	5.46	5.41	5.28	5.69	5.61	5.53	5.76	5.75
$1B_{2g}$	$(2b_{3g} \rightarrow 3d_{xy})$	5.69	5.48	5.45	5.33	5.70	5.62	5.57	5.80	5.80
$3A_g$	$(2b_{3g} \rightarrow 3d_{yz})$	5.82	5.55	5.66	5.53	5.82	5.81	5.77	6.00	6.02
$2B_{2g}$	$(2b_{2g} \rightarrow 3s)$	6.37	5.94	5.83	5.65	6.37	6.09	5.99	6.13	6.13
$2B_{1u}$	$(2b_{3g} \rightarrow 4p_y)$	6.10	5.91	5.91	5.78	6.10	6.00	5.97	6.27	6.29
$2A_u$	$(2b_{3g} \rightarrow 4p_x)$	6.13	5.94	5.93	5.81	6.13	6.03	6.00	6.29	6.30

methods, SOPPA and SOPPA(CCSD), the excitation energies become even smaller and the deviation from the reference values thus again larger. Adding the noniterative second order correction of CIS(D), on the other hand, leads also to an improvement over the CIS results, but the changes are smaller than in RPA(D), which implies that the result are all larger than the CCSDR(3) reference values and for three out of four in better agreement. At the CC2 level the deviations are even more reduced. However, the CC2 results are scattered around the reference values contrary to the CIS(D) and CCSD results which are all above. Furthermore they are either as close as the CIS(D) or CCSD results to the CCSDR(3) results or even closer.

For the Rydberg states we also observe again, that the RPA and CIS results are almost identical with one exception, the $4A_1$ state. RPA and CIS gives also excitation energies, which are in better agreement with the CCSDR(3) values than all other methods apart from CCSD, which in most but not all cases is closer to the CCSDR(3) results than RPA or CIS. Inclusion of the noniterative doubles corrections in RPA(D) and CIS(D) destroys this good agreement with CCSD and CCSDR(3). The same happens also for almost all states at the level of the iterative second order methods SOPPA and CC2. The deviations are smaller, however, in CIS(D) and CC2 than in RPA(D) and SOPPA. RPA(D) underestimates thus the reference values with approximately -0.29 ± 0.10 eV, SOPPA with -0.30 ± 0.11 eV and SOPPA(CCSD) with -0.44 ± 0.11 eV, whereas CIS(D) with -0.28 ± 0.23 eV and CC2 with -0.21 ± 0.1 eV.

Anthracene. Only two excitations in each irreducible representation were calculated which gives 7 valence and 9 Rydberg states. The excitations are listed in ascending order of the CCSDR(3) method for each type of transition in Table 5. The transitions to the s, d_{z^2}, and $d_{x^2-y^2}$ Rydberg orbitals are mixed since they all transform as the same irreducible representation. This makes the characterization of these transformations some what unclear. There are no $\pi \rightarrow \pi^*$ transitions among the two lowest states of every irreducible representation. From the work of Bak et al.,[10] we know that $\pi \rightarrow \pi^*$ transitions do not occur for SOPPA and RPA before the third state in each irreducible representation. The weight of the single excitations, % R_1, in the CCSD excitation energy calculations is ~95% for all

Rydberg states, whereas the valence states, and in particular the $1B_{3u}$ and $1B_{1g}$ states with only 91% and the $2A_g$ states with only 90%, have smaller weights.

Similar to the other molecules, we observe large differences between the different valence states. The order of the two lowest valence states $1B_{3u}$ and $1B_{2u}$, e.g., is not reproduced by all second-order methods. RPA, SOPPA, SOPPA(CCSD), CIS, and CC2 all predict the $1B_{2u}$ to be the lowest valence state contrary to CCSDR(3), whereas RPA(D), CIS(D) and CCSD predict the same order of states as CCSDR(3). The CIS(D) value for the lowest valence transition, $1B_{3u}$, is even in good agreement with the CCSDR(3) energy. The CCSDR(3) results for these two transitions differ by only 0.045 eV, which is within the range of uncertainty of the CCSDR(3) calculations compared to CC3.[115] In the work of Kawashima et al.[125] using multireference Møller−Plesset theory (MRMP) the two transitions are discussed for benzene, naphthalene, anthracene and naphthacene. For anthracene they found also $1B_{3u}$ to be the lowest excited state. They state furthermore, that the permutation of the two excited states first occurs at the level of naphthacene. Experiment[153] seems to favor the $1B_{2u}$ as the lowest state but the $1B_{3u}$ transition is hard to measure and therefore quite uncertain.[125] The second B_{3u} valence state, on the other hand, is predicted too low relative to CCSDR(3) by all methods but CCSD. Finally, RPA, CIS and even CCSD have the two lowest B_{1g} states interchanged compared to CCSDR(3). RPA(D), SOPPA, and SOPPA(CCSD) do not suffer from this problem, but still predict the $2B_{1g}$ state too low relative to the $2B_{2u}$ state. For the Rydberg states we observe only a problem with the $2B_{2g}$ state which is by all methods but SOPPA, SOPPA(CCSD), and CCSD, placed to high relative to the other states.

In general the deviations from the CCSDR(3) results are again on average much larger for the valence states as for the Rydberg states. The RPA results are scattered around the CCSDR(3) values with a span of more than 1.5 eV. Addition of the noniterative second order correction in RPA(D) reduces all valence excitation energies, so that they are now all smaller than at the CCSDR(3) level. The spread of deviations, on the other hand, is significantly reduced to 0.5 eV. This trend is continued on going to the iterative second order method SOPPA, where the span of deviations is only 0.3 eV but all excitation energies are even lower than in RPA(D). SOPPA(CCSD) finally gives the lowest valence excitation energies with a maximal deviation from CCSDR(3) of 1 eV and a spread of 0.45 eV.

CIS gives again always larger excitation energies than RPA and thus with one exception higher values than CCSDR(3). Addition of the noniterative second order corrections in CIS(D) leads to partially very large reductions so that the CIS(D) results are now scattered around the CCSDR(3) values with deviations within ±0.1 eV. Going to CC2 reduces the excitation energies even further but only marginally leading to smaller values than at the CCSDR(3) level for all but one valence state. CCSD, finally, gives for all valence states larger energies than CCSDR(3). However, CCSD is only in 2 out of 7 states in better agreement with CCSDR(3) than CC2 and even CIS(D), while CIS(D) gives a better agreement than CC2 for 4 of the 7 states. A particular large difference between CCSD and CCSDR(3) is found for the $1B_{1g}$ state, which has a relatively large contribution from doubles excitations.

For the Rydberg states the picture changes again entirely with the exception of the $2B_{2g}$ state, which has a very large double excitation contribution and which does not follow the trend of the other Rydberg states. Therefore it will not be discussed further here. CCSD gives basically the same results as CCSDR(3) for all Rydberg states. The RPA and CIS results are again equal and in better agreement with the reference values than all other methods apart from CCSD. Adding the noniterative second order corrections in RPA(D) and CIS(D) reduces all excitation energies and leads thus to a less favorable agreement with CCSDR(3). This trend continues to the iterative second order methods. Nevertheless, CC2, SOPPA, and SOPPA(CCSD) yield quite satisfying results with deviations from CCSDR(3) which all lie within a span of 0.1 eV for CC2, 0.04 eV for SOPPA, and 0.03 eV for SOPPA(CCSD) but approximately −0.22 eV (CC2), −0.34 eV (SOPPA), and −0.48 eV (SOPPA(CCSD)) displaced from the reference.

Phenanthrene. For phenanthrene we have included five states in each irreducible representation in this study. This gives rise to 8 valence states, 11 Rydberg states, and one mixed valence/Rydberg state, the $5A_1$ state. Comparison with experimental results shows that for this state the CCSDR(3) vertical excitation energy is 0.35 eV higher than the absorption maximum.[159] The results are shown in Table 6 in ascending order of the CCSDR(3) results. The weight of the single excitations, $\% R_1$, in the CCSD excitation energy calculations is 95% for all Rydberg states, whereas the valence states, and in particular the $2A_1$ and $2B_2$ states with only 91%, have smaller weights.

Compared to anthracene we observe less problems with the order of the valence states for phenanthrene and they are all in the A_1 irreducible representation. RPA and CIS predict the $2A_1$ and the $3A_1$ valence states too high. Addition of the noniterative double contribution corrects this problem for the $2A_1$ state but not for the $3A_1$ state. Furthermore SOPPA, SOPPA(CCSD) and CIS(D) predict the $6A_1$ state too low compared to the $4B_2$ which at the CCSDR(3) level is almost degenerate with it. For the Rydberg transitions we find only one case, where RPA(D) and CIS(D) overestimate the doubles correction for the $4A_2$ Rydberg state relative to the $4B_1$ Rydberg state so that these two states come in the wrong order at the RPA(D) and CIS(D) level.

The RPA and CIS valence energies are all but one ($1B_2$) or two ($1B_2$ and $5A_1$), respectively, larger than the CCSDR(3) reference values. Addition of the noniterative doubles correction reduces all excitation energies with the exception of the $1B_2$ state in CIS(D). The RPA(D) energies are thus smaller than the reference values with the exception of the $3A_1$ which comes out too high as mentioned already. For four of the nine valence states the RPA results are thus in better agreement with the reference values than the second order propagator methods. For the other five states RPA(D) gives again results closest to CCSDR(3), whereas the SOPPA (with the exception of the $4B_2$ state) and the SOPPA(CCSD) results are increasingly too small. The $4B_2$ state, on the other hand, is remarkably close to the reference energy for SOPPA and SOPPA(CCSD) compared to other valence transitions. The CIS(D) valence excitation energies are scattered around the reference values. The $3A_1$ state shows a unusual large deviation from CCSDR(3) at the CIS level which is reduced but still quite large at the CIS(D) level. The CC2 results are mainly smaller than the reference values, whereas the CCSD results are all larger. In five out of the nine valence states the CC2 results are also again in better agreement with CCSDR(3) results than the CCSD excitation energies.

Similar to the other PAH molecules we find that the Rydberg transitions are significantly better described. The CCSD results are within +0.03 eV of the CCSDR(3) values closely followed by the almost identical RPA and CIS results, which are atmost 0.16 eV too large. For the other methods we observe also the usual pattern with the CIS(D), CC2, RPA(D), SOPPA, and SOPPA(CCSD) energies being 0.16 ± 0.07 eV, 0.21 ± 0.04

TABLE 6: Phenanthrene: Vertical Singlet Excitation Energies (in eV) in Ascending Order of CCSDR(3) Energies

	state	RPA	RPA(D)	SOPPA	SOPPA(CCSD)	CIS	CIS(D)	CC2	CCSD	CCSDR(3)
					Valence $\pi\pi^*$					
$2A_1$	$(4b_1 \rightarrow 11b_1)$	4.68	3.59	3.45	3.18	4.88	4.07	4.04	4.10	4.02
$1B_2$	$(4b_1 \rightarrow 7a_2)$	4.46	4.78	4.15	3.94	4.78	5.01	4.70	4.87	4.81
$2B_2$	$(3a_2 \rightarrow 12b_1)$	5.82	4.79	4.49	4.26	5.88	5.17	5.06	5.10	5.02
$3A_1$	$(3a_2 \rightarrow 7a_2)$	6.09	5.35	4.61	4.38	6.44	5.88	5.10	5.51	5.27
$3B_2$	$(3a_2 \rightarrow 11b_1)$	5.66	4.82	4.79	4.53	6.05	5.38	5.32	5.60	5.44
$4A_1$	$(4b_1 \rightarrow 12b_1)$	5.73	5.41	5.03	4.85	6.22	6.04	5.49	5.83	5.61
$5A_1$	$(4b_1 \rightarrow 7a_2/3p_z)$	6.16	5.74	5.85	5.72	5.91	5.75	5.90	6.11	6.03
$4B_2$	$(3a_2 \rightarrow 9b_1)$	6.36	5.94	6.12	5.96	6.39	6.13	6.06	6.27	6.24
$6A_1$	$(2a_2 \rightarrow 7a_2)$	6.98	6.02	5.54	5.34	6.62	6.04	6.13	6.31	6.24
					Rydberg $\pi\pi^*$					
$5B_2$	$(4b_1 \rightarrow 3d_{xz})$	6.53	6.19	6.16	6.02	6.53	6.32	6.25	6.52	6.50
					Rydberg $\pi\sigma^*$					
$1B_1$	$(4b_1 \rightarrow 3d_{z^2})$	5.56	5.22	5.17	5.05	5.56	5.39	5.32	5.51	5.48
$1A_2$	$(3a_2 \rightarrow 3d_{z^2})$	5.88	5.46	5.42	5.28	5.89	5.63	5.57	5.75	5.73
$2B_1$	$(4b_1 \rightarrow 3p_y)$	5.89	5.50	5.47	5.35	5.89	5.66	5.61	5.83	5.80
$2A_2$	$(4b_1 \rightarrow 3p_x)$	6.04	5.60	5.57	5.45	6.04	5.76	5.71	5.92	5.90
$3B_1$	$(3a_2 \rightarrow 3p_x)$	6.23	5.80	5.76	5.62	6.23	5.96	5.90	6.11	6.10
$3A_2$	$(3a_2 \rightarrow 3p_y)$	6.28	5.86	5.79	5.65	6.28	6.01	5.92	6.14	6.13
$4B_1$	$(4b_1 \rightarrow 3d_{z^2})$	6.35	6.03	5.98	5.86	6.35	6.17	6.10	6.34	6.32
$4A_2$	$(4b_1 \rightarrow 3d_{xy})$	6.42	5.96	5.98	5.86	6.42	6.09	6.10	6.34	6.32
$5B_1$	$(4b_1 \rightarrow 3p_y)$	6.42	6.00	6.01	5.89	6.43	6.13	6.13	6.35	6.34
$5A_2$	$(3a_2 \rightarrow 3d_{z^2})$	6.62	6.21	6.19	6.04	6.62	6.35	6.31	6.53	6.53

TABLE 7: Biphenylene: Vertical Singlet Excitation Energies (in eV) in Ascending Order of CCSDR(3) Energies

	state	RPA	RPA(D)	SOPPA	SOPPA(CCSD)	CIS	CIS(D)	CC2	CCSD	CCSDR(3)
					Valence $\pi\pi^*$					
$1B_{3g}$	$(2b_{2g} \rightarrow 5b_{1g})$	3.63	3.57	3.13	2.90	3.87	3.92	3.69	3.91	3.83
$1B_{1u}$	$(2b_{2g} \rightarrow 6b_{3u})$	4.48	3.51	3.32	3.07	4.69	3.97	3.88	3.97	3.89
$2A_g$	$(1b_{1g} \rightarrow 5b_{1g})$	5.99	4.85	4.60	4.40	6.19	5.46	5.18	5.22	5.12
$2B_{1u}$	$(1a_u \rightarrow 5b_{1g})$	6.09	5.08	4.93	4.70	6.40	5.75	5.56	5.84	5.68
$2B_{3g}$	$(1a_u \rightarrow 6b_{3u})$	6.33	5.64	5.38	5.21	6.60	6.09	5.85	6.14	5.99
$1B_{2u}$	$(2b_{3u} \rightarrow 5b_{1g})$	8.02	5.96	5.85	5.70	7.93	6.46	6.38	6.62	6.30
$2B_{2u}$	$(2b_{2g} \rightarrow 2a_u)$	6.14	6.32	5.64	5.49	6.43	6.67	6.10	6.49	6.32
$4A_g$	$(2b_{3u} \rightarrow 6b_{3u})$	8.33	6.30	6.11	5.96	8.45	6.68	6.55	6.99	6.74
					Rydberg $\pi\sigma^*$					
$1B_{2g}$	$(2b_{2g} \rightarrow 3s, d)$	5.15	4.80	4.75	4.62	5.15	4.98	4.90	5.11	5.09
$1B_{3u}$	$(2b_{2g} \rightarrow 3p_z)$	5.56	5.19	5.14	5.02	5.56	5.35	5.28	5.52	5.50
$1A_u$	$(2b_{2g} \rightarrow 3p_y)$	5.60	5.23	5.20	5.08	6.89	5.38	5.33	5.57	5.56
$2B_{2g}$	$(2b_{2g} \rightarrow 3s, d)$	5.92	5.61	5.58	5.45	5.92	5.75	5.69	5.95	5.94
$1B_{1g}$	$(2b_{2g} \rightarrow 3d_{yz})$	6.04	5.68	5.65	5.52	6.04	5.80	5.76	6.03	6.02
$3B_{2g}$	$(2b_{2g} \rightarrow 3s, d)$	6.04	5.75	5.75	5.62	6.04	5.88	5.85	6.10	6.10
$2A_u$	$(1a_u \rightarrow 3s, d)$	6.67	6.10	6.01	5.93	6.67	6.25	6.15	6.37	6.32
$4B_{2g}$	$(2b_{2g} \rightarrow 5s, d)$	6.28	6.01	6.00	5.87	6.28	6.11	6.06	6.38	6.39
$3A_u$	$(2b_{2g} \rightarrow 4p_y)$	6.41	6.11	6.13	6.00	6.41	6.20	6.18	6.52	6.52
$2B_{3u}$	$(2b_{2g} \rightarrow 4p_z)$	6.43	6.14	6.13	6.01	6.44	6.23	6.19	6.52	6.54
$2B_{1g}$	$(1a_u \rightarrow 3p_z)$	7.00	6.39	6.36	6.28	7.00	6.55	6.50	6.73	6.70
$3B_{1g}$	$(2b_{2g} \rightarrow 3d_{yz})$	6.63	6.32	6.32	6.19	6.63	6.39	6.36	6.71	6.70
$5B_{2g}$	$(2b_{2g} \rightarrow 4s, d)$	6.60	6.32	6.31	6.18	6.60	6.38	6.35	6.70	6.71
					Rydberg $\pi\pi^*$					
$3B_{1u}$	$(2b_{2g} \rightarrow 3p_x)$	5.67	5.41	5.42	5.28	5.68	5.56	5.47	5.72	5.69
$3A_g$	$(2b_{2g} \rightarrow 3d_{xz})$	6.13	5.74	5.85	5.72	6.09	5.75	5.93	6.20	6.21
$3B_{3g}$	$(2b_{2g} \rightarrow 4d_{xy})$	6.15	5.89	5.91	5.77	6.15	6.02	5.98	6.26	6.26
$4B_{1u}$	$(2b_{2g} \rightarrow 4p_x)$	6.44	6.17	6.18	6.05	6.46	6.06	6.23	6.55	6.57
$5A_g$	$(2b_{3u} \rightarrow 5d_{xz})$	6.65	6.37	6.38	6.25	6.65	6.44	6.41	6.76	6.77
$4B_{3g}$	$(2b_{2g} \rightarrow 5d_{xy})$	6.65	6.38	6.38	6.25	6.67	6.35	6.42	6.77	6.79

eV, 0.31 ± 0.05 eV, 0.33 ± 0.02 eV, and 0.46 ± 0.03 eV, respectively, below the reference values.

Biphenylene. The results for the 27 lowest states of biphenylene are shown in Table 7. They consist of 8 valence, 13 Ry $\pi\sigma^*$, and 6 Ry $\pi\pi^*$ states. The weight of the single excitations, % R_1, in the CCSD excitation energy calculations is 95% or more for all Rydberg states, whereas the valence states, and in particular the $1B_{1u}$ and $2A_g$ states with only 91% and the $1B_{2u}$ states with only 90%, have smaller weights.

Concerning the order of the valence states, we find that all but the RPA(D) and CIS(D) methods have the two lowest B_{2u} valence states interchanged compared to CCSDR(3). From the literature one knows that the two B_{2u} states are near degenerate excitations, and using Platt's model, they are expected to combine to yield a plus an minus state.[123,163] RPA(D) predicts also the $1B_{1u}$ and the $4A_g$ valence states too low relative to the other valence states. All methods have also interchanged the $2B_{1g}$ and $3B_{1g}$ Rydberg states compared to CCSDR(3). At the

TABLE 8: Deviations in Excitation Energies of the Calculated Valence $\pi\pi^*$ Singlet Excited States with Respect to CCSDR(3)

	RPA	RPA(D)	SOPPA	SOPPA(CCSD)	CIS	CIS(D)	CC2	CCSD	MR-CISD
number of states	39	39	39	39	39	39	39	39	11
mean	0.40	−0.30	−0.55	−0.76	0.60	0.08	−0.07	0.13	0.44
std. dev.	0.55	0.19	0.17	0.22	0.51	0.19	0.10	0.08	0.26
abs. mean	0.51	0.31	0.55	0.76	0.63	0.17	0.11	0.13	0.44
maximum	1.72	−0.80	−0.87	−1.21	1.71	0.61	−0.22	0.32	0.90

TABLE 9: Deviations in Excitation Energies of the Calculated Rydberg $\pi\pi^*$ and $\pi\sigma^*$ Singlet Excited States with Respect to CCSDR(3)

	RPA/CIS	RPA(D)	SOPPA	SOPPA(CCSD)	CIS(D)	CC2	CCSD	MR-CISD
number of states	76	76	76	76	76	76	76	21
mean	−0.01	−0.32	−0.34	−0.46	−0.20	−0.22	0.00	0.13
std. dev.	0.11	0.06	0.04	0.05	0.10	0.06	0.02	0.13
abs. mean	0.09	0.32	0.34	0.46	0.20	0.22	0.02	0.14
maximum	0.35	−0.57	−0.41	−0.55	−0.51	−0.37	0.09	0.51

CCSDR(3) level these states are degenerate, because their energy difference is less than 0.01 eV. Furthermore all other methods than CCSD predict the $2A_u$ Rydberg state too high relative to the other Rydberg states.

For the valence states on biphenylene, we observe the same trends as for the other PAH molecules. The RPA and CIS results show a very large span of deviations from the CCSDR(3) results. The CIS results are always larger than the CCSDR(3) results and with only one exception, the $1B_{2u}$ state, also larger than the RPA results. Consequently they are in the majority of valence states in worse agreement with the CCSDR(3) results. Addition of the noniterative second order correction reduces in almost all cases the excitation energies by up to 2 eV in the case of RPA(D) and always slightly less in CIS(D). The RPA(D) energies are thus always smaller than the CCSDR(3) results whereas most CIS(D) results are still larger than the CCSDR(3) results. The spread of deviations, on the other hand, is significantly reduced compared to RPA or CIS. This trend, lowering of the excitation energies and narrowing of the spread of deviations, is continued again on going to SOPPA and CC2. The SOPPA and CC2 results exhibit therefore the same span of deviations, 0.15 eV, from the CCDSR(3) results, but the SOPPA excitation energies are about 0.5 eV lower than the CC2 energies. On going from SOPPA to SOPPA(CCSD) the excitation energies become again even smaller and the spread of difference from the reference values is slightly increased. Going from CC2 to CCSD, on the other hand, leads to an increase in energy of all valence exited states, which are then all above the CCSDR(3) reference values. But only for two of the 8 valence states are the CCSD values closer to the reference values than the CC2 results.

For the Rydberg states we observe the usual picture with the exception of the $2A_u$ and $2B_{1g}$ states, which differ significantly from other Rydberg states at least at the RPA, CIS, RPA(D), and CIS(D) levels of theory. In general, we find again that the CCSD and CCSDR(3) as well as RPA and CIS predict essentially the same excitation energies. Futhermore, with the exception of the above-mentioned states, the RPA and CIS give the second best agreement with the CCSDR(3) reference values only surpassed by CCSD. Addition of the noniterative or iterative doubles corrections in RPA(D), CIS(D), SOPPA, CC2, or SOPPA(CCSD) destroys this good agreement step by step. Contrary to other molecules however, the RPA(D) (or CIS(D)) Rydberg excitation energies are not always in better agreement with the CCSDR(3) reference values than the SOPPA (or CC2) values. The deviations are 0.35 ± 0.13 eV, 0.34 ± 0.07 eV, 0.29 ± 0.22 eV, and 0.27 ± 0.18 eV for RPA(D), SOPPA, CIS(D), and CC2, respectively. SOPPA(CCSD) finally gives again the lowest energies and thus the largest deviations from the reference values with 0.47 ± 0.07 eV.

Discussion and Statistical Evaluation

In the discussion of the results of the individual PAH molecules it became clear that there is a fundamental difference between the performance of the different methods for valence and Rydberg states. The weight of the single excitations, % R_1, for the Rydberg states is e.g. ≈95% in the CCSD calculations, whereas it is consistently lower for the valence states. Therefore we have collected statistical data for all methods separately for the valence and Rydberg states in Table 8 and Table 9.

Valence $\pi\pi^*$ Transitions. At one end of the scale of methods, we find the RPA and CIS methods, which do not only lead to the largest deviations from the CCSDR(3) results, 1.7 eV, as well as the second (0.63 eV) and fourth (0.51 eV) largest absolute mean deviations for the dominant valence states but also exhibit much larger spans of deviations from the reference values as indicated by their standard deviations, 0.5 eV, in Table 8. The accuracy of the results depends thus very much on the state. The CIS results are mostly larger than the CCSDR(3) results and with only few exceptions also larger than the RPA results. Consequently, they are in the majority of valence states in worse agreement with the CCSDR(3) results, which is also reflected in the larger mean deviations in Table 8. As consequence of the inconsistent treatment of different valence states, these methods exhibit also frequently problems with the ordering of valence states.

Inclusion of the noniterative second order corrections in RPA(D) or CIS(D) totally changes this picture. It repairs often the problems with the order of states, i.e. the noniterative doubles corrections have the ability to correct the RPA or CIS energies enough to resemble the order of the CCSDR(3) energies. Furthermore they give much more homogeneous deviations from CCSDR(3). The maximum and spread of deviations from the CCSDR(3) results are now less than half of what is found for RPA and CIS and approximately only twice as large as for CC2 or CCSD. Also the mean deviations are significantly smaller. However, this is more pronounced for CIS(D) than for RPA(D), because the changes due to the noniterative corrections are smaller in CIS(D) than in RPA(D). Consequently the excitation energies are always larger at the CIS(D) level than at the RPA(D) level, Figure 7, and all but three RPA(D) results are smaller than the CCSDR(3) results, Figures 2 and 4, whereas the CIS(D) values are scattered around the reference values with a preference for larger values, Figures 2 and 5. In the majority

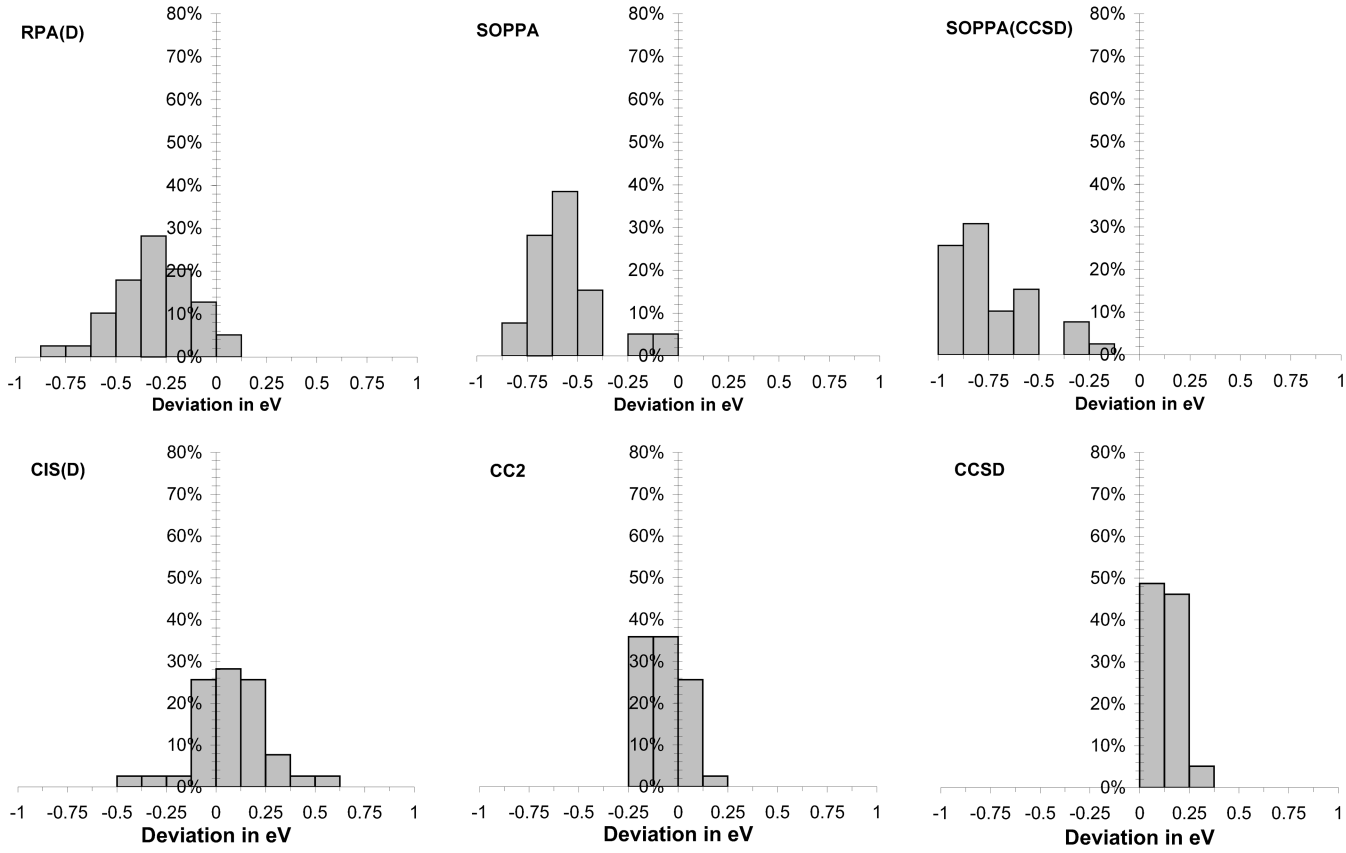

Figure 2. Histogram of the frequency of deviation (from CCSDR(3) in %) of the calculated RPA(D) (top left), SOPPA (top middle), SOPPA(CCSD) (top right), CIS(D) (bottom left), CC2 (bottom middle), and CCSD (bottom right) valence $\pi\pi^*$ singlet excited states.

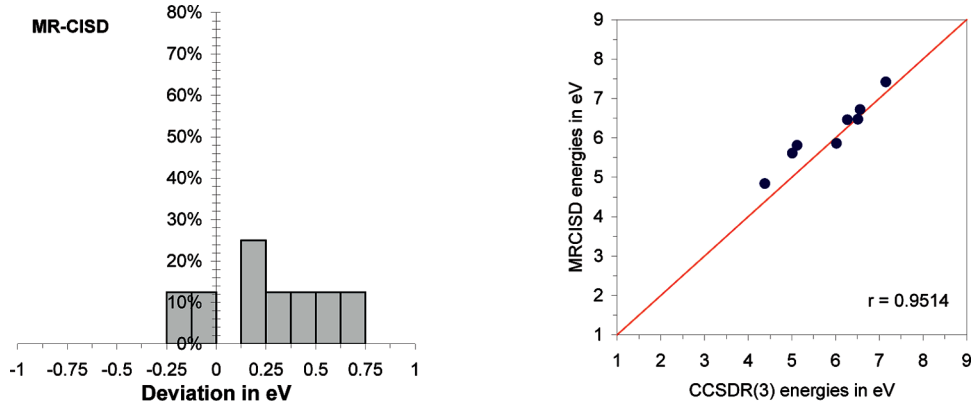

Figure 3. MR-CISD versus CCSDR(3): histogram (left) of the frequency of deviation (in %) from CCSDR(3) and correlation plot (right) for valence $\pi\pi^*$ singlet excited states.

of cases the CIS(D) results are thus closer to the CCSDR(3) reference values as shown by the mean deviation in Table 8. The spread of results, however, is similar, which implies that the RPA(D) results are simply moved by about 0.3−0.4 eV to lower energies as shown also in the correlation plot between RPA(D) and CIS(D), Figure 7.

The iterative second-order methods usually reproduce the spectrum qualitatively. However, even SOPPA, SOPPA(CCSD), or CC2 are sometimes not able to reproduce the correct order of states. This happens mainly in cases where the states are very close lying in energy at the CCSDR(3) level.

The MP based iterative methods exhibit in general larger deviations from the CCSDR(3) values than the CC based methods and perform increasingly worse in the series RPA(D), SOPPA, and SOPPA(CCSD). SOPPA and SOPPA(CCSD) predict excitation energies, which are all lower than the CCSDR(3) results (on average by 0.55 and 0.76 eV) with the SOPPA(CCSD) energies being even smaller than the SOPPA energies, Figure 6, combined with a larger span of deviations 0.22 eV. RPA(D), on the other hand, gives often larger excitation energies than SOPPA, Figure 6, and thus results in better agreement with the CCSDR(3) reference values. Overall, RPA(D) exhibit the smaller mean deviation (−0.30 eV) but a larger spread of deviations as indicated by the standard deviation, 0.19 eV, in Table 8 and the correlation plots in Figure 4.

Contrary to the MP based methods, we find for the CC-based methods that the agreement with the CCSDR(3) reference results is clearly improved on going from the noniterative method CIS(D) to the iterative methods CC2 and CCSD as shown by the absolute mean errors (0.17, 0.11, and 0.13) and standard deviations in Table 8. Whereas CIS(D) and CC2 give results which are scattered around the CCSDR(3) reference values, we

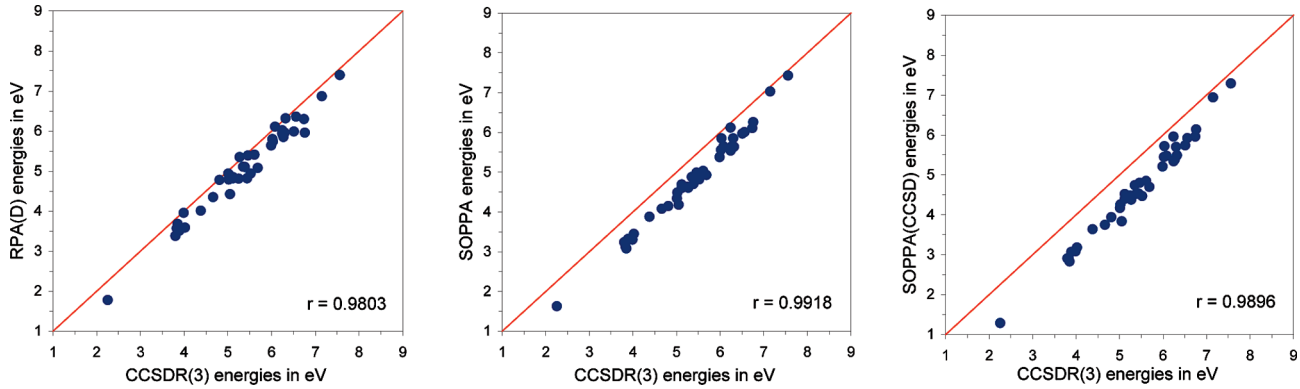

Figure 4. Correlation plots for valence $\pi\pi^*$ singlet excited states: RPA(D) (left), SOPPA (middle), and SOPPA(CCSD) (right) versus CCSDR(3).

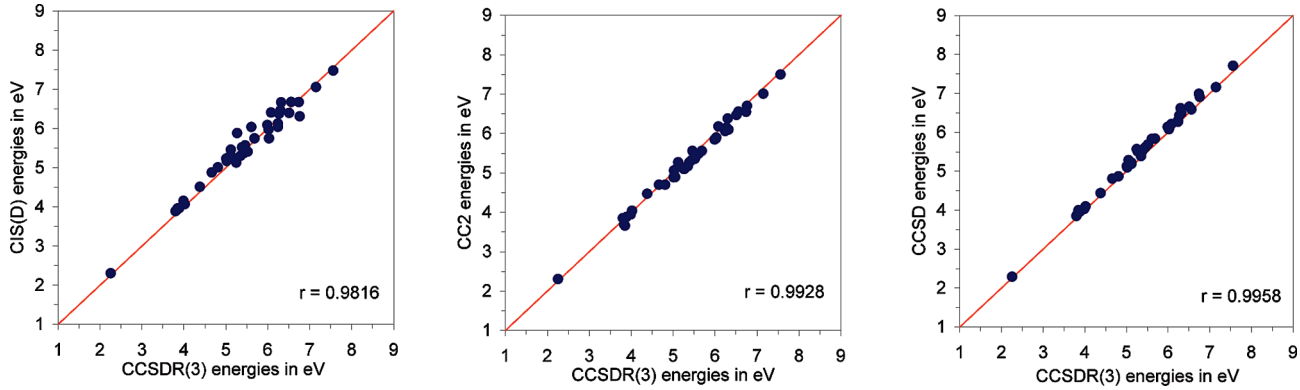

Figure 5. Correlation plots for valence $\pi\pi^*$ singlet excited states: CIS(D) (left), CC2 (middle), and CCSD (right) versus CCSDR(3).

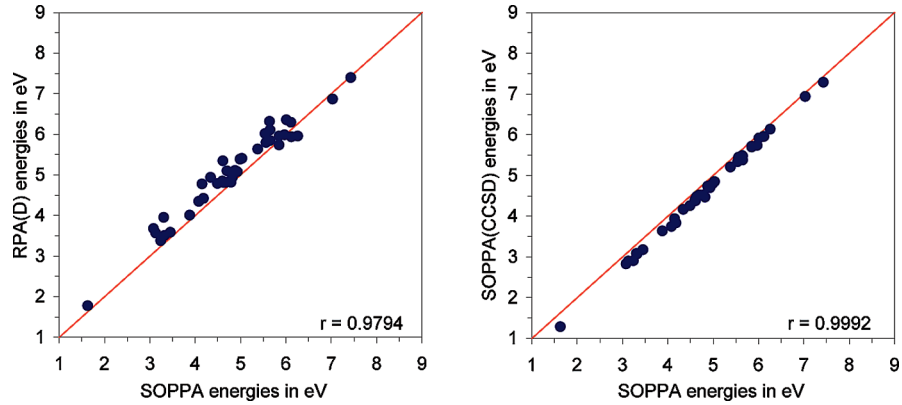

Figure 6. Correlation plots for valence $\pi\pi^*$ singlet excited states: RPA(D) (left) and SOPPA(CCSD) (right) versus SOPPA.

observe that the CCSD excitation energies are always larger than the CCSDR(3) values, Figures 2 and 5, which implies that the noniterative triples correction to the valence states is negative. In the previous studies by Thiel and co-workers,[113,115] this was found to be the case for the majority of states studied there. Comparing the CC2 and CCSD results we find also like in the previous studies[113,115] that for the majority, 25 of the 39 valence states, CC2 gives results closer to the CCSDR(3) results than CCSD. On average the CC2 results are thus closer to the CCSDR(3) results as shown by the lower (absolute) mean deviations and have the smaller largest deviation, Table 8. However, the deviations of the CC2 results are more spread out as shown in Figures 2 and 5 and quantified by the larger standard deviation in Table 8. It is thus not straightforward to say whether the CC2 or CCSD results for the valence states should be considered to be in better agreement with the CCSDR(3) reference values in general.

The number of states calculated at the MR-CISD level is too small for generally valid statements, but we can observe that they are on average in better agreement with the reference values than the bare CIS results but not necessarily than the CIS(D) results, Figure 3.

Rydberg $\pi\pi^*$ and $\pi\sigma^*$ Transitions. In the statistical evaluation in Table 9 and the histograms and correlation plots in Figures 8−12, we have only included the 76 states (21 in the case of MR-CISD) which exhibit a dominant Rydberg character. This implies that the $2B_{1g}$ state of naphthalene was excluded.

First of all one notices that all methods perform significantly better and much more consistently in the calculation of Rydberg transitions with partially smaller mean deviations, RPA/CIS, SOPPA, SOPPA(CCSD), CCSD, and MR-CISD and a smaller spread of deviations for all methods. Second RPA and CIS

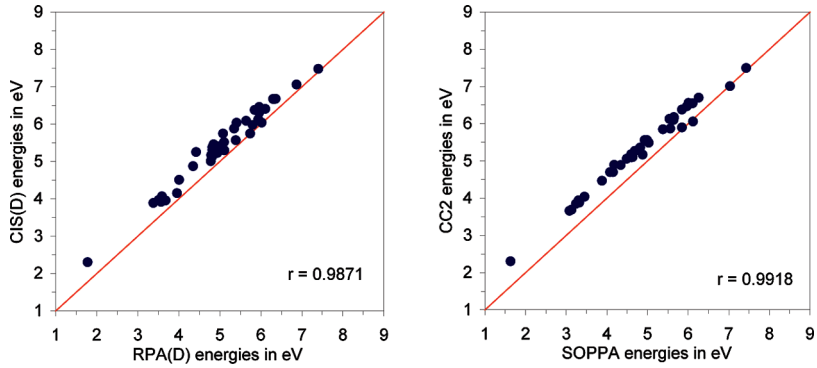

Figure 7. Correlation plots for valence $\pi\pi^*$ singlet excited states: CIS(D) versus RPA(D) (left) and CC2 versus SOPPA (right).

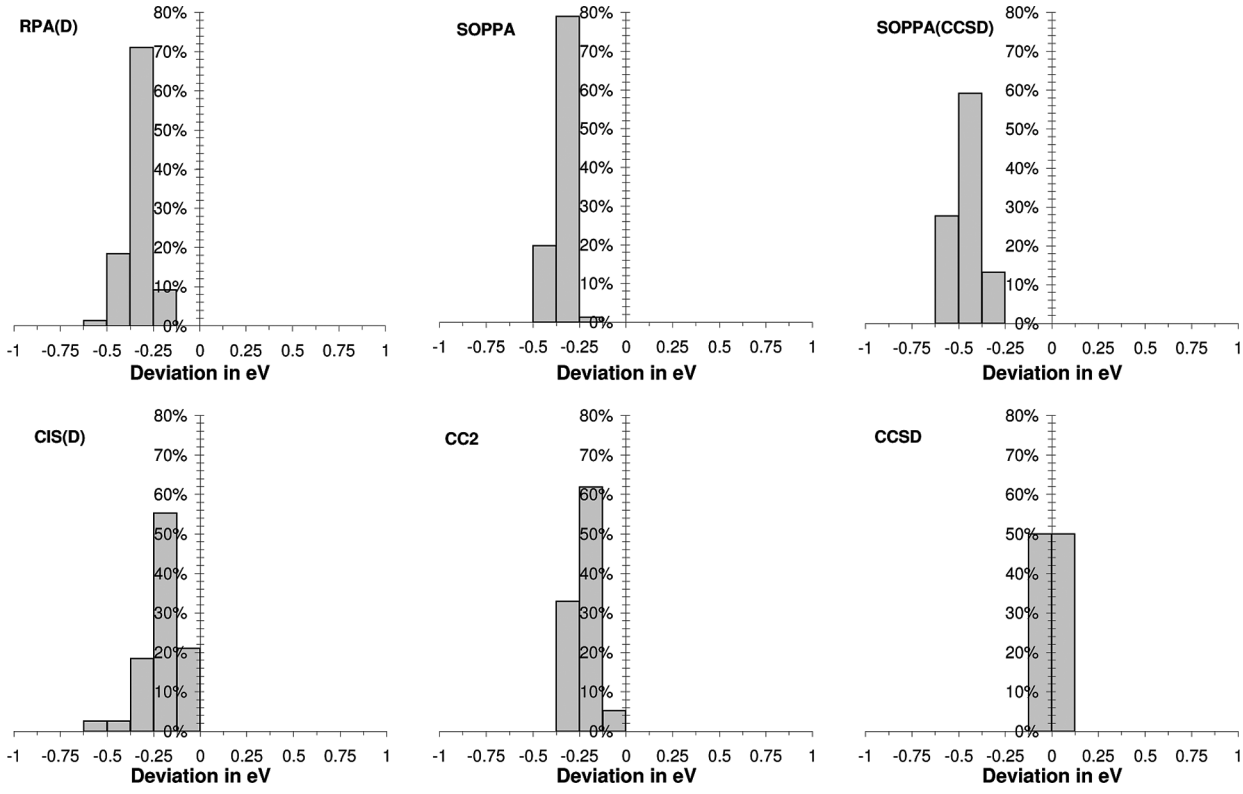

Figure 8. Histogram of the frequency of deviation (from CCSDR(3) in %) of the calculated RPA(D) (top left), SOPPA (top middle), SOPPA(CCSD) (top right), CIS(D) (bottom left), CC2 (bottom middle) and CCSD (bottom right) Rydberg $\pi\pi^*$ and $\pi\sigma^*$ singlet excited states.

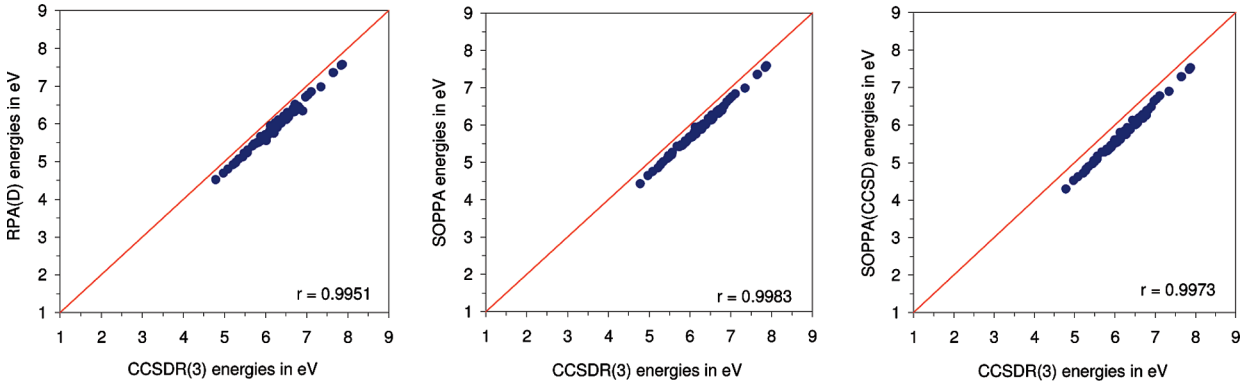

Figure 9. Correlation plots for the Rydberg $\pi\pi^*$ and $\pi\sigma^*$ singlet excited states: RPA(D) (left), SOPPA (middle), and SOPPA(CCSD) (right) versus CCSDR(3).

produce essentially identical results for all Rydberg states quite contrary to the valence states.

All three indicators, Table 9 and Figures 8 and 10, show that the CCSD results essentially reproduce the CCDSR(3) results for the whole set of 76 Ry states with deviations of less than 0.1 eV. The mean and absolute mean deviation are 0.02 eV or less with a standard deviation of only 0.02 eV. For the Rydberg transitions CCSD is thus clearly the best second-order method

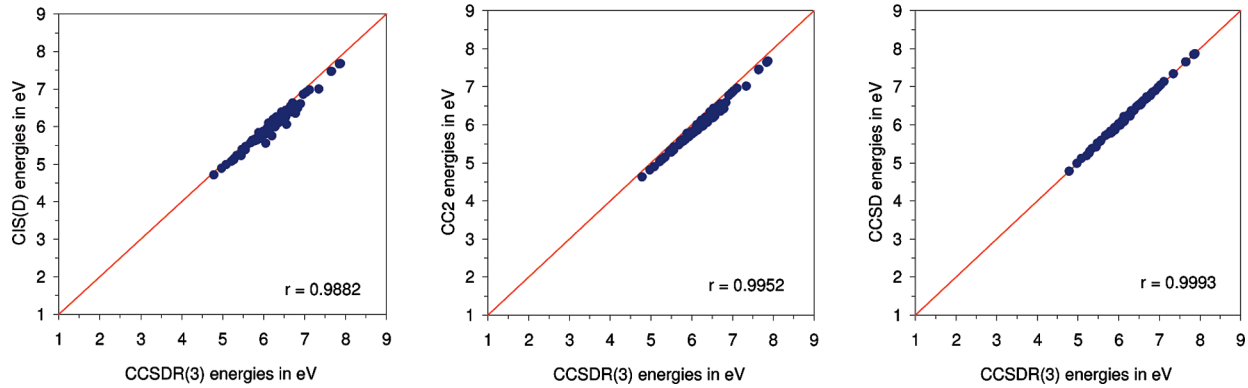

Figure 10. Correlation plots for the Rydberg $\pi\pi^*$ and $\pi\sigma^*$ singlet excited states: CIS(D) (left), CC2 (middle), and CCSD (right) versus CCSDR(3).

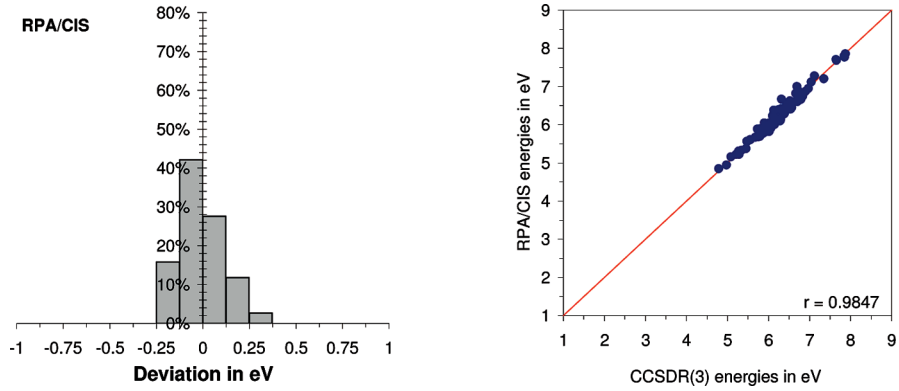

Figure 11. RPA and CIS versus CCSDR(3): histogram (left) of the frequency of deviation (in %) from CCSDR(3) and correlation plot (right) for Rydberg $\pi\pi^*$ and $\pi\sigma^*$ singlet excited states.

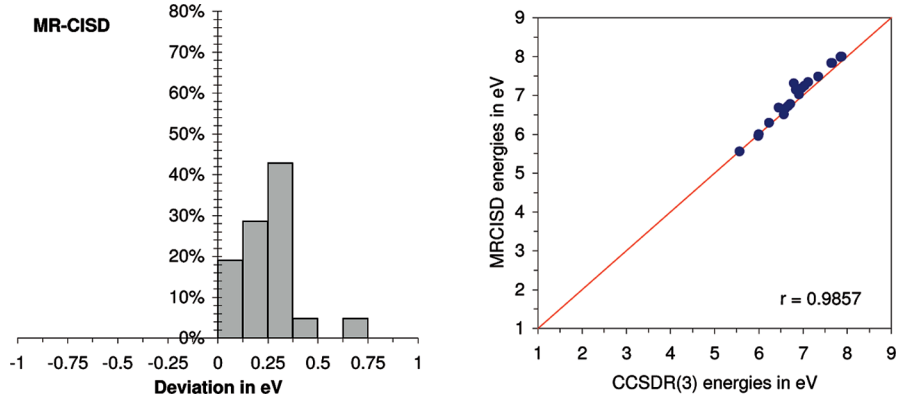

Figure 12. MR-CISD versus CCSDR(3): histogram (left) of the frequency of deviation (in %) from CCSDR(3) and correlation plot (right) for Rydberg $\pi\pi^*$ and $\pi\sigma^*$ singlet excited states.

contrary to the valence states and the CCSD energies are rather symmetrically distributed around the reference values.

Surprisingly, RPA and CIS reproduce the majority of the CCSDR(3) excitation energies to the Ryberg states better than all the other methods apart from CCSD. They lead to the second smallest mean (absolute mean) deviation, −0.01 eV (0.09 eV), from the reference results and more or less symmetric distribution around the CCSDR(3) values, Figure 11. However despite this small mean deviation, these methods exhibit a larger spread of deviations as shown in Figure 11 and documented by the largest standard deviation of all methods, 0.11 eV.

Inclusion of electron correlation at the level of the noniterative or iterative second order methods improves the consistency of the results compared to RPA/CIS, as indicated by the falling standard deviations, but also reduces the excitation energies significantly, so that RPA(D), SOPPA, SOPPA(CCSD), CIS(D), and CC2 underestimate all CCSDR(3) excitation energies to the Rydberg states, Figures 8−10. This leads to a less favorable agreement with CCSDR(3) as compared to RPA/CIS or CCSD.

SOPPA, e.g., predicts the Rydberg states on average 0.34 ± 0.04 eV too low as compared to CCSDR(3), whereas RPA(D) gives slightly larger values for the energies, Figure 13, as well as for the standard deviation, i.e., an average error of −0.32 ± 0.06 eV. This implies that RPA(D) performs again slightly better but less consistently than SOPPA. SOPPA(CCSD), on the other hand, gives even smaller excitation energies with an average deviation of −0.46 ± 0.05 eV, Figure 13, and is thus also slightly less consistent than SOPPA.

Similar to the MP based methods but contrary to the valence states, we observe for the Rydberg states that CIS(D) [−0.20 ± 0.10 eV] performs slightly better than CC2 [−0.22 ± 0.06

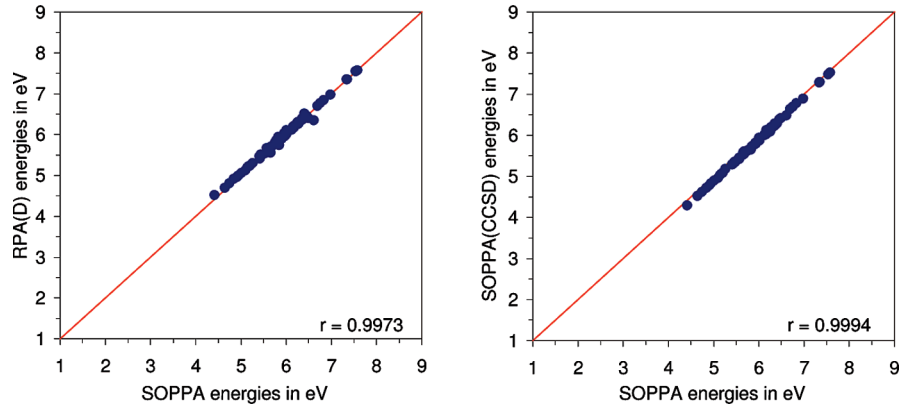

Figure 13. Correlation plots for Rydberg $\pi\pi^*$ and $\pi\sigma^*$ singlet excited states: RPA(D) (left) and SOPPA(CCSD) (right) versus SOPPA.

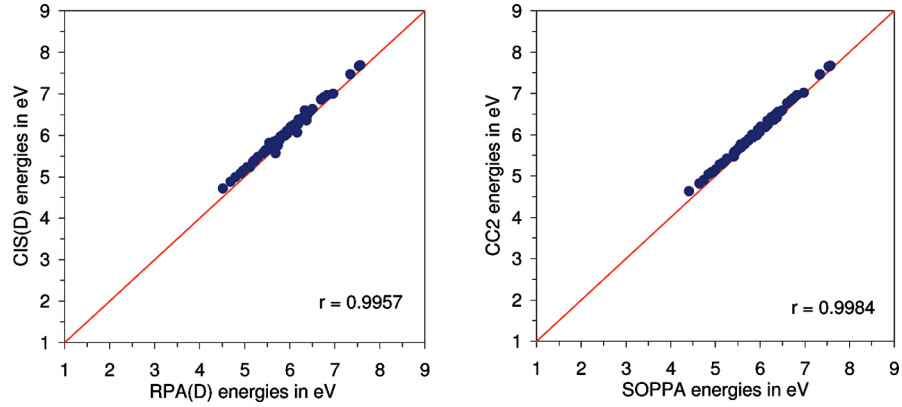

Figure 14. Correlation plots for Rydberg $\pi\pi^*$ and $\pi\sigma^*$ singlet excited states: CIS(D) versus RPA(D) (left) and CC2 versus SOPPA (right).

eV] on average but is less consistent. Both methods are, however significantly less accurate than CCSD for the Rydberg transitions.

In general, the MP based linear response methods RPA(D) and SOPPA predict on average the excitation energies to be about 0.12 eV lower than their CC based analogs, Figure 14, but are slightly more consistent as shown by their smaller standard deviations.

The MR-CISD results for the 21 Ry states studied, Figure 12, are again all larger than the reference CCSDR(3) values. However, contrary to the valence states the agreement is much better so that only CCSD and CIS/RPA exhibit smaller mean deviations.

Summary

We have carried out a systematic comparison of several second order methods for the calculation of vertical electronic excitation energies in polycyclic aromatic hydrocarbons and benchmarked them against the noniterative third order method CCSDR(3). First of all we find that there seems to be a fundamental difference between excitations to valence and to Rydberg states, which leads to significant differences in the performance of the methods for the two types of excitation energies and that all methods perform in some way better for the Rydberg states than for the valence states.

Our further findings we can summarize as follows:

• For the valence states CC2 reproduces on average the CCSDR(3) results more closely than CCSD as was seen previously by Thiel and co-workers.[113,115] For the Rydberg transitions, on the other hand, we observe, that CC2 performs consistently worse than CCSD and on average even somewhat worse than CIS(D).

• Comparing the Møller−Plesset perturbation theory based linear response methods, RPA(D) and SOPPA, with their coupled cluster based CC analogs, CIS(D) and CC2, we find that the coupled cluster methods give in general higher excitation energies and lead thus to a better agreement with the CCSDR(3) reference. This is more pronounced for the valence states, but can also be seen for the Rydberg transitions. The span of deviations of the MP based methods and their CC analogs is rather similar, so that one can say the results of the MP based methods are essentially just moved to lower energies.

• RPA(D) leads to the smaller mean deviations from the reference values than SOPPA but is less consistent. Nevertheless one can say that RPA(D) performs on average better than SOPPA for the states studied here. The results of SOPPA(CCSD) calculations, on the other hand, are always in worse agreement with CCSDR(3) results than the SOPPA results. The deviations of the SOPPA(CCSD) results follow the SOPPA results with respect to which transitions are reproduced poorly. This is not surprising in itself, but the CCSD amplitudes used in SOPPA(CCSD) were expected to improve on the Møller−Plesset amplitudes used in SOPPA and thus on the excitation energies. The latter is surely not the case for the PAH molecules. SOPPA(CCSD) does-not improve the results of SOPPA, on the contrary it is less consistent and gives even lower energies.

• Quite unexpected we observe finally that for the Rydberg states RPA and CIS give essentially the same results and that on average they reproduce the CCSDR(3) values better than all second-order methods apart from CCSD.

However, one should keep in mind that we have only investigated one particular type of organic chromophore, polycyclic aromatic hydrocarbons. The conclusions of this study for the valence states should therefore be tested on a more diverse

set of chromophores as, e.g., the one recently suggested by Thiel and co-workers.[113−115]

Acknowledgment. The authors thank Drs. J. Kongsted and O. Christiansen for helpful discussions. S.P.A.S. acknowledges grants from the Danish Natural Science Research Council/The Danish Councils for Independent Research, from the Carlsberg foundation, from the Danish Center for Scientific Computing and support from the COST action CM0805.

References and Notes

(1) Linderberg, J.; Öhrn, Y. *Propagators in Quantum Chemistry*; Academic Press: London, 1973.

(2) Jørgensen, P.; Simons, J. *Second Quantization-Based Methods in Quantum Chemistry*; Academic Press: New York, 1981.

(3) Olsen, J.; Jørgensen, P. Time-dependent response theory with applications to self-consistent field and multiconfigurational self-consistent field wave functions. In *Modern Electronic Structure Theory*; Yarkony, D. R., Ed.; World Scientific: Singapore, 1995; Chapter 13, pp 857−990.

(4) Rowe, D. J. Equations-of-Motion Method and the Extended Shell Model. *Rev. Mod. Phys.* **1968**, *40*, 153–166.

(5) Dalgaard, E. Time-dependent multiconfigurational Hartree-Fock theory. *J. Chem. Phys.* **1980**, *72*, 816–823.

(6) Olsen, J.; Jørgensen, P. Linear and nonlinear response functions for an exact state and for an MCSCF state. *J. Chem. Phys.* **1985**, *82*, 3235–3264.

(7) Nielsen, E. S.; Jørgensen, P.; Oddershede, J. Transition moments and dynamic polarizabilities in a second order polarization propagator approach. *J. Chem. Phys.* **1980**, *73*, 6238–6246.

(8) Packer, M. J.; Dalskov, E. K.; Enevoldsen, T.; Jensen, H. J. A.; Oddershede, J. A new implementation of the second order polarization propagator approximation (SOPPA): The excitation spectra of benzene and naphthalene. *J. Chem. Phys.* **1996**, *105*, 5886–5900.

(9) Christiansen, O.; Bak, K. L.; Koch, H.; Sauer, S. P. A. A Second-order doubles correction to excitation energies in the random phase approximation. *Chem. Phys. Lett.* **1998**, *284*, 47–62.

(10) Bak, K. L.; Koch, H.; Oddershede, J.; Christiansen, O.; Sauer, S. P. A. Atomic integral driven second order polarization propagator calculations of the excitation spectra of naphthalene and anthracene. *J. Chem. Phys.* **2000**, *112*, 4173–4185.

(11) Åstrand, P.-O.; Ramanujam, P. S.; Hvilsted, S.; Bak, K. L.; Sauer, S. P. A. Ab initio calculation of the electronic spectra of azobenzene dyes and its impact on the design of optical data storage materials. *J. Am. Chem. Soc.* **2000**, *122*, 3482–3487.

(12) Nielsen, C. B.; Sauer, S. P. A.; Mikkelsen, K. V. Response theory in the multipole reaction field model for equilibrium and nonequilibrium solvation: Exact theory and the second order polarization propagator approximation. *J. Chem. Phys.* **2003**, *119*, 3849–3870.

(13) Olsen, J.; Jørgensen, P.; Helgaker, T.; Oddershede, J. Quadratic response functions in a second-order polarization propagator framework. *J. Phys. Chem. A* **2005**, *109*, 11618–11628.

(14) Geertsen, J.; Oddershede, J. A coupled cluster polarization propagator method applied to CH^+. *J. Chem. Phys.* **1986**, *85*, 2112–2118.

(15) Geertsen, J.; Eriksen, S.; Oddershede, J. Some aspects of the coupled cluster based polarization propagator method. *Adv. Quantum Chem.* **1991**, *22*, 167–209.

(16) Sauer, S. P. A. Second Order Polarization Propagator Approximation with Coupled Cluster Singles and Doubles Amplitudes - SOPPA(CCSD): The Polarizability and Hyperpolarizability of Li-. *J. Phys. B: At. Mol. Opt. Phys.* **1997**, *30*, 3773–3780.

(17) Dalskov, E. K.; Sauer, S. P. A. Correlated, static and dynamic polarizabilities of small molecules. A comparison of four black box methods. *J. Phys. Chem. A* **1998**, *102*, 5269–5274.

(18) Monkhorst, H. J. Calculation of Properties with the Coupled-Cluster Method. *Int. J. Quantum Chem. Symp.* **1977**, *11*, 421–432.

(19) Mukherjee, D.; Mukherjee, P. K. A response-function approach to the direct calculation of the transition-energy in a multiple-cluster expansion formalism. *Chem. Phys.* **1979**, *39*, 325–335.

(20) Ghosh, S.; Mukherjee, D.; Bhattacharyya, S. N. A spin-adapted linear response theory in a coupled-cluster framework for direct calculation of spin-allowed and spin-forbidden transition energies. *Chem. Phys. Lett.* **1982**, *72*, 161–176.

(21) Dalgaard, E.; Monkhorst, H. J. Some aspects of the time-dependent coupled-cluster approach to dynamic response functions. *Phys. Rev. A* **1983**, *28*, 1217–1222.

(22) Koch, H.; Jørgensen, P. Coupled cluster response function. *J. Chem. Phys.* **1990**, *93*, 3333–3344.

(23) Koch, H.; Jensen, H. J. A.; Jørgensen, P.; Helgaker, T. Excitation-Energies from the Coupled Cluster Singles and Doubles Linear Response Function (CCSDLR) - Applications to Be, CH^+, CO, and H_2O. *J. Chem. Phys.* **1990**, *93*, 3345–3350.

(24) Stanton, J. F.; Bartlett, R. J. The equation of motion coupled-cluster method. A systematic biorthogonal approach to molecular excitation energies, transition probabilities, and excited state properties. *J. Chem. Phys.* **1993**, *98*, 7029–7039.

(25) Datta, B.; Sen, P.; Mukherjee, D. Coupled-Cluster Based Linear Response Approach to Property Calculations: Dynamic Polarizability and Its Static Limit. *J. Phys. Chem.* **1995**, *99*, 6441–6451.

(26) Christiansen, O.; Koch, H.; Jørgensen, P. The second-order approximate coupled cluster singles and doubles model CC2. *Chem. Phys. Lett.* **1995**, *243*, 409–418.

(27) Christiansen, O.; Koch, H.; Jørgensen, P. Response functions in the CC3 iterative triple excitation model. *J. Chem. Phys.* **1995**, *103*, 7429–7441.

(28) Koch, H.; Christiansen, O.; Jørgensen, P.; Sanchez de Merás, A. M.; Helgaker, T. The CC3 model: An iterative coupled cluster approach including connected triples. *J. Chem. Phys.* **1997**, *106*, 1808–1818.

(29) Hald, K.; Hättig, C.; Yeager, D. L.; Jørgensen, P. Linear response CC2 triplet excitation energies. *Chem. Phys. Lett.* **2000**, *328*, 291–301.

(30) Hald, K.; Hättig, C.; Jørgensen, P. Triplet excitation energies in the coupled cluster singles and doubles model using an explicit triplet spin coupled excitation space. *J. Chem. Phys.* **2000**, *113*, 7765–7772.

(31) Hald, K.; Jørgensen, P.; Olsen, J.; Jaszunski, M. An analysis and implementation of a general coupled cluster approach to excitation energies with application to the B2 molecule. *J. Chem. Phys.* **2001**, *115*, 671–679.

(32) Hald, K.; Hättig, C.; Olsen, J.; Jørgensen, P. CC3 triplet excitation energies using an explicit spin coupled excitation space. *J. Chem. Phys.* **2001**, *115*, 3545–3552.

(33) Sattelmeyer, K. W.; Stanton, J. F.; Olsen, J.; Gauss, J. A comparison of excited state properties for iterative approximate triples linear response coupled cluster methods. *Chem. Phys. Lett.* **2001**, *347*, 499–504.

(34) Sekino, H.; Bartlett, R. J. A linear response, coupled-cluster theory for excitation energy. *Int. J. Quantum Chem. Symp.* **1984**, *18*, 255.

(35) Geertsen, J.; Rittby, M.; Bartlett, R. J. The Equation-of-Motion Coupled-Cluster Method: Excitation Energies of Be and CO. *Chem. Phys. Lett.* **1989**, *164*, 57–62.

(36) Stanton, J. F.; Bartlett, R. J. The equation of motion coupled-cluster method. A systematic biorthogonal approach to molecular excitation energies, transition probabilities, and excited state properties. *J. Chem. Phys.* **1993**, *98*, 7029–7039.

(37) Comeau, D. C.; Bartlett, R. J. The equation-of-motion coupled-cluster method. Applications to open- and closed-shell reference states. *Chem. Phys. Lett.* **1993**, *207*, 414–423.

(38) Piecuch, P.; Bartlett, R. J. EOMXCC: A new coupled-cluster method for electronic excited states. *Adv. Quantum Chem.* **1999**, *34*, 295–380.

(39) Kowalski, K.; Piecuch, P. Excited-state potential energy curves of CH^+: a comparison of the EOMCCSDt and full EOMCCSDT results. *Chem. Phys. Lett.* **2001**, *347*, 237–246.

(40) Kowalski, K.; Piecuch, P. The active-space equation-of-motion coupled-cluster methods for excited electronic states: Full EOMCCSDt. *J. Chem. Phys.* **2001**, *115*, 643–651.

(41) Kucharski, S. A.; Włoch, M.; Musiał, M.; Bartlett, R. J. Coupled-cluster theory for excited electronic states: The full equation-of-motion coupled-cluster single, double, and triple excitation method. *J. Chem. Phys.* **2001**, *115*, 8263–8266.

(42) Hirata, S. Higher-order equation-of-motion coupled-cluster methods. *J. Chem. Phys.* **2004**, *121*, 51–59.

(43) Kállay, M.; Gauss, J. Calculation of excited-state properties using general coupled-cluster and configuration-interaction models. *J. Chem. Phys.* **2004**, *121*, 9257–9269.

(44) Smith, C. E.; King, R. A.; Crawford, T. D. Coupled cluster methods including triple excitations for excited states of radicals. *J. Chem. Phys.* **2005**, *122*, 54110.

(45) Bartlett, R. J.; Musial, M. Coupled-Cluster theory in quantum chemistry. *Rev. Mod. Phys.* **2007**, *79*, 291–352.

(46) Musiał, M.; Bartlett, R. J. Addition by subtraction in coupled cluster theory. II. Equation-of-motion coupled cluster method for excited, ionized, and electron-attached states based on the nCC ground state wave function. *J. Chem. Phys.* **2007**, *127*, 24106.

(47) Emrich, K. An Extension of the Coupled Cluster Formalism to Excited States (I). *Nucl. Phys. A* **1981**, *351*, 379–396.

(48) Christiansen, O. Coupled cluster theory with emphasis on selected new developments. *Theor. Chem. Acc.* **2006**, *116*, 106–123.

(49) Krylov, A. I. Equation-of-Motion Coupled-Cluster Methods for Open-Shell and Electronically Excited Species: The Hitchhiker's Guide to Fock Space. *Annu. Rev. Phys. Chem.* **2008**, *59*, 433–462.

(50) Larsen, H.; Hald, K.; Olsen, J.; Jørgensen, P. Triplet excitation energies in full configuration interaction and coupled-cluster theory. *J. Chem. Phys.* **2001**, *115*, 3015–3020.

(51) Watts, J. D.; Bartlett, R. J. The inclusion of connected triple excitations in the equation-of-motion coupled-cluster method. *J. Chem. Phys.* **1994**, *101*, 3073–3078.

(52) Watts, J. D.; Bartlett, R. J. Economical triple excitation equation-of-motion coupled-cluster methods for excitation energies. *Chem. Phys. Lett.* **1995**, *233*, 81–87.

(53) Watts, J. D.; Gwaltney, S. R.; Bartlett, R. J. Couplet-cluster calculations of the excitation energies of ethylene, butadiene, and cyclopentadiene. *J. Chem. Phys.* **1996**, *105*, 6979–6988.

(54) Watts, J. D.; Bartlett, R. J. Equation-of-motion coupled-cluster calculations of excitation energies. The challenge of ozone. *Spectrochim. Acta A* **1999**, *55*, 495–507.

(55) Christiansen, O.; Koch, H.; Jørgensen, P. Perturbative triple excitation corrections to coupled cluster singles and doubles excitation energies. *J. Chem. Phys.* **1996**, *105*, 1451–1459.

(56) Christiansen, O.; Koch, H.; Jørgensen, P.; Olsen, J. Excitation energies of H_2O, N_2 and C_2 in full configuration interaction and coupled cluster theory. *Chem. Phys. Lett.* **1996**, *256*, 185–194.

(57) Hirata, S.; Nooijen, M.; Grabowski, I.; Bartlett, R. Perturbative corrections to coupled-cluster and equation-of-motion coupled-cluster energies: A determinantal analysis. *J. Chem. Phys.* **2001**, *114*, 3919–3928.

(58) Hirata, S.; Nooijen, M.; Grabowski, I.; Bartlett, R. Perturbative corrections to coupled-cluster and equation-of-motion coupled-cluster energies: A determinantal analysis (vol 114, p 3919, 2001). *J. Chem. Phys.* **2001**, *115*, 3967–3968.

(59) Piecuch, P.; Kowalski, K.; Pimienta, I.; McGuire, M. Recent advances in electronic structure theory: Method of moments of coupled-cluster equations and renormalized coupled-cluster approaches. *Int. Rev. Phys. Chem.* **2002**, *21*, 527–655.

(60) Piecuch, P.; Kowalski, K.; Pimienta, I.; Fan, P.; Lodriguito, M.; McGuire, M.; Kucharski, S.; Kus, T.; Musiał, M. Method of moments of coupled-cluster equations: a new formalism for designing accurate electronic structure methods for ground and excited states. *Theo. Chem. Acc.* **2004**, *112*, 349–393.

(61) Kowalski, K.; Piecuch, P. New coupled-cluster methods with singles, doubles, and noniterative triples for high accuracy calculations of excited electronic states. *J. Chem. Phys.* **2004**, *120*, 1715–1738.

(62) Włoch, M.; Gour, J.; Kowalski, K.; Piecuch, P. Extension of renormalized coupled-cluster methods including triple excitations to excited electronic states of open-shell molecules. *J. Chem. Phys.* **2005**, *122*, 214107.

(63) Fan, P.-D.; Kowalski, K.; Piecuch, P. Non-iterative corrections to extended coupled-cluster energies employing the generalized method of moments of coupled-cluster equations. *Mol. Phys.* **2005**, *103*, 2191–2213.

(64) Łoch, M. W.; Lodriguito, M. D.; Piecuch, P.; Gour, J. R. Two new classes of non-iterative coupled-cluster methods derived from the method of moments of coupled-cluster equations. *Mol. Phys.* **2006**, *104*, 2149–2172.

(65) Shiozaki, T.; Hirao, K.; Hirata, S. Second- and third-order triples and quadruples corrections to coupled-cluster singles and doubles in the ground and excited states. *J. Chem. Phys.* **2007**, *126*, 244106.

(66) Kowalski, K.; Valiev, M. Noniterative Corrections to Equation-of-Motion Coupled-Cluster Excited State Energies Based on the Reduced Method of Moments of Coupled Cluster Equations. *Int. J. Quantum Chem.* **2008**, *108*, 2178–2190.

(67) Hättig, C.; Weigand, F. CC2 excitation energy calculations on large molecules using the resolution of the identity approximation. *J. Chem. Phys.* **2000**, *113*, 5154–5161.

(68) Hättig, C. Geometry optimizations with the coupled-cluster model CC2 using the resolution-of-the-identity approximation. *J. Chem. Phys.* **2003**, *118*, 7751–7761.

(69) Köhn, A.; Hättig, C. Analytic gradients for excited states in the coupled-cluster model CC2 employing the resolution-of-the-identity approximation. *J. Chem. Phys.* **2003**, *119*, 5021–5036.

(70) Hättig, C. Structure optimizations for excited states with correlated second-order methods: CC2 and ADC(2). *Adv. Quantum Chem.* **2005**, *50*, 37–60.

(71) Sauer, S. P. A.; Oddershede, J. Correlated Polarization Propagator Calculations of Static Dipole Polarizabilities. *Int. J. Quantum Chem.* **1994**, *50*, 317–332.

(72) Paidarová, I.; Sauer, S. P. A. Calculations of Dipole and Quadrupole Polarizability Radial Functions for LiH and HF: A Comparison of Different Linear Response Methods. *Adv. Quantum Chem.* **2005**, *48*, 185–208.

(73) Packer, M. J.; Sauer, S. P. A.; Oddershede, J. Correlated dipole oscillator sum rules. *J. Chem. Phys.* **1994**, *100*, 8969–8975.

(74) Sauer, S. P. A.; Paidarová, I. Correlated linear response calculations of the C6 dispersion coefficients of hydrogen halides. *Comput. Lett.* **2007**, *3*, 399–421.

(75) Paidarová, I.; Sauer, S. P. A. A comparison of Møller-Plesset and coupled cluster linear response theory methods for the calculation of dipole oscillator strength sum rules and C6 dispersion coefficients. *Collect. Czech. Chem. Commun.* **2008**, *73*, 1415–1436.

(76) Sauer, S. P. A.; Enevoldsen, T.; Oddershede, J. Paramagnetism of closed shell diatomic hydrides with six valence electrons. *J. Chem. Phys.* **1993**, *98*, 9748–9757.

(77) Sauer, S. P. A.; Ogilvie, J. F. Experimental and Theoretical Estimates of the Rotational g Factor of AlH in the Electronic Ground State $X^1\Sigma^+$. *J. Phys. Chem.* **1994**, *98*, 8617–8621.

(78) Sauer, S. P. A. Theoretical Estimate of the Rotational g-Factor, Magnetizability and Electric Dipole Moment of GaH. *Chem. Phys. Lett.* **1996**, *260*, 271–279.

(79) Sauer, S. P. A. The Rotational g Tensor of HF, H_2O, NH_3 and CH_4: A Comparison of Correlated Ab Initio Methods. *Adv. Quantum Chem.* **2005**, *48*, 468–490.

(80) Enevoldsen, T.; Oddershede, J.; Sauer, S. P. A. Correlated Calculations of Indirect Nuclear Spin-Spin Coupling Constants using Second Order Polarization Propagator Approximations: SOPPA and SOPPA(CCSD). *Theor. Chem. Acc.* **1998**, *100*, 275–284.

(81) Sauer, S. P. A.; Raynes, W. T. Unexpected differential sensitivity of nuclear spin-spin coupling constants to bond stretching in BH_4^-, NH_4^+ and SiH_4. *J. Chem. Phys.* **2000**, *113*, 3121–3129.

(82) Grayson, M.; Sauer, S. P. A. The computation of Karplus equation coefficients and their components using self-consistent field and second order polarization propagator methods. *Mol. Phys.* **2000**, *98*, 1981–1990.

(83) Sauer, S. P. A.; Raynes, W. T.; Nicholls, R. A. Nuclear spin-spin coupling in silane and its isotopomers: ab initio calculation and experimental investigation. *J. Chem. Phys.* **2001**, *115*, 5994–6006.

(84) Ligabue, A.; Sauer, S. P. A.; Lazzeretti, P. Correlated and Gauge Invariant Calculations of Nuclear Magnetic Shielding Constants Using the Continuous Transformation of the Origin of the Current Density Approach. *J. Chem. Phys.* **2003**, *118*, 6830–6845.

(85) Head-Gordon, M.; Rico, R. J.; Oumi, M.; Lee, T. J. A doubles correction to electronic excited states from configuration interaction in the space of single substitutions. *Chem. Phys. Lett.* **1994**, *219*, 21–29.

(86) Foresman, J. B.; Head-Gordon, M.; Pople, J. A.; Frisch, M. J. Toward a Systematic Molecular Orbital Theory for Excited States. *J. Phys. Chem.* **1992**, *96*, 135–149.

(87) Brown, F. B.; Shavitt, I.; Shepard, R. Multireference configuration interaction treatment of potential energy surfaces: symmetric dissociation of H_2O in a double-zeta basis. *Chem. Phys. Lett.* **1984**, *105*, 363–369.

(88) Bruna, P. J.; Peyerimhoff, S. D. Excited-State Potentials. In *Ab Initio Methods in Quantum Chemistry - I. Advances in Chemical Physics*; Lawley, K. P., Ed.; John Wiley & Sons Ltd.: Chichester, U.K., 1987; pp 1−97.

(89) Roos, B. O. The complete active space self-consistent field method and its application in electronic structure calculations. In *Ab Initio Methods in Quantum Chemistry - II. Advances in Chemical Physics*; Lawley, K. P., Ed.; John Wiley & Sons Ltd.: Chichester, U.K., 1987; pp 399−445.

(90) Mogensen, B. J.; Rettrup, S. Average Virtual Orbitals in Configuration Interaction Studies with Application to the Low-Lying Singlet States of the Carbon Monoxide and Acetone Molecules. *Int. J. Quantum Chem.* **1992**, *44*, 1045–1056.

(91) Palmieri, P.; Tarroni, R.; Rettrup, S. Hartree-Fock Operators to Improve Virtual Orbitals and Configuration Interaction Energies. *J. Chem. Phys.* **1994**, *100*, 5849–5856.

(92) Rettrup, S.; Mogensen, B. J. Optimized Virtual Orbitals for the Calculation of Molecular Properties of Excited Electronic States. *Strongly Corr. Electron Syst. Chem., Experiment Theory* **1996**, 55–66.

(93) Oddershede, J.; Jørgensen, P.; Beebe, N. H. F. Analysis of excitation energies and transition moments. *J. Phys. B* **1978**, *11*, 1–15.

(94) Swanstrøm, P.; Jørgensen, P. An open shell polarization propagator: Doublet-doublet transitions. *J. Chem. Phys.* **1979**, *71*, 4652–4660.

(95) Oddershede, J.; Sabin, J. R.; Diercksen, G. H. F.; Grüner, N. E. The structure and spectrum of SiC_2. *J. Chem. Phys.* **1985**, *83*, 1702–1708.

(96) Oddershede, J.; Grüner, N. E.; Diercksen, G. H. F. Comparison between equation of motion and polarization propagator calculations. *Chem. Phys.* **1985**, *97*, 303–310.

(97) Sabin, J. R.; Oddershede, J.; Diercksen, G. H. F.; Grüner, N. E. The calculated electronic excitation spectra of Si_2C and Si_3. *J. Chem. Phys.* **1986**, *84*, 354–360.

(98) Scuseria, G. E.; Geertsen, J.; Oddershede, J. Electronic spectra and response properties of BH and AlH. *J. Chem. Phys.* **1989**, *90*, 2338–2343.

(99) Koch, H.; Christiansen, O.; Jørgensen, P.; Olsen, J. Excitation energies of BH, CH_2 and Ne in the full configuration interaction and the hierarchy CCS, CC2, CCSD and CC3 of coupled cluster methods. *Chem. Phys. Lett.* **1995**, *244*, 75–82.

(100) Pecul, M.; Jaszunski, M.; Larsen, H.; Jørgensen, P. Singlet excited states of Be_2. *J. Chem. Phys.* **2000**, *112*, 3671–3679.

(101) Larsen, H.; Olsen, J.; Jørgensen, P.; Christiansen, O. Full configuration interaction benchmarking of coupled-cluster models for the lowest singlet energy surfaces of N_2. *J. Chem. Phys.* **2000**, *113*, 6677–6686.

(102) Cronstrand, P.; Christiansen, O.; Norman, P.; Ågren, H. Theoretical calculations of excited state absorption. *Phys. Chem. Chem. Phys.* **2000**, *2*, 5357–5363.

(103) Åstrand, P.-O.; Sommer-Larsen, P.; Hvilsted, S.; Ramanujam, P. S.; Bak, K. L.; Sauer, S. P. A. Five-member rings as diazo components in optical data storage devices: An ab initio investigation of the lowest singlet excitation energies. *Chem. Phys. Lett.* **2000**, *325*, 115–119.

(104) Christiansen, O.; Jørgensen, P. The Electronic Spectrum of Furan. *J. Am. Chem. Soc.* **1998**, *120*, 3423–3430.

(105) Christiansen, O.; Gauss, J.; Stanton, J. F.; Jørgensen, P. The electronic spectrum of pyrrole. *J. Chem. Phys.* **1999**, *111*, 525–537.

(106) Christiansen, O.; Koch, H.; Halkier, A.; Jørgensen, P.; Helgaker, T.; Sánchez de Merás, A. Large-scale calculations of excitation energies in coupled cluster theory: The singlet excited states of benzene. *J. Chem. Phys.* **1996**, *105*, 6921–6939.

(107) Öhrn, A.; Christiansen, O. Electronic excitation energies of pyrimidine studied using coupled cluster response theory. *Phys. Chem. Chem. Phys.* **2001**, *3*, 730–740.

(108) Cronstrand, P.; Christiansen, O.; Norman, P.; Ågren, H. Ab initio modeling of excited state absorption of polyenes. *Phys. Chem. Chem. Phys.* **2001**, *3*, 2567–2575.

(109) Köhn, A.; Hättig, C. On the nature of the low-lying singlet states of 4-(dimethyl-amino)benzonitrile. *J. Am. Chem. Soc.* **2004**, *126*, 7399–7410.

(110) Osted, A.; Kongsted, J.; Christiansen, O. Theoretical Study of the Electronic Gas-Phase Spectrum of Glycine, Alanine, and Related Amines and Carboxylic Acids. *J. Phys. Chem. A* **2005**, *109*, 1430–1440.

(111) Stanton, J. F.; Gauss, J. The first excited singlet state of s-tetrazine: A theoretical analysis of some outstanding questions. *J. Chem. Phys.* **1996**, *104*, 9859–9869.

(112) Pastore, M.; Angeli, C.; Cimiraglia, R. A multireference perturbation theory study on the vertical electronic spectrum of thiophene. *Theor. Chem. Acc.* **2007**, *118*, 35–46.

(113) Schreiber, M.; Silva-Junior, M. R.; Sauer, S. P. A.; Thiel, W. Benchmarks for electronically excited states: CASPT2, CC2, CCSD, and CC3. *J. Chem. Phys.* **2008**, *128*, 134110.

(114) Silva-Junior, M. R.; Schreiber, M.; Sauer, S. P. A.; Thiel, W. Benchmarks for electronically excited states: TD-DFT and DFT/MRCI. *J. Chem. Phys.* **2008**, *129*, 104103.

(115) Sauer, S. P. A.; Schreiber, M.; Silva-Junior, M. R.; Thiel, W. Benchmarks for electronically excited states: A comparison of noniterative and iterative triples corrections in linear response coupled cluster methods - CCSDR(3) versus CC3. *J. Chem. Theory Comput.* **2009**, *5*, 555–564.

(116) Martin, J. M. L.; El-Yazal, J.; Francois, J.-P. Structure and Vibrational Spectrum of Some Polycyclic Aromatic Compounds Studied by Density Functional Theory. 1. Naphthalene, Azulene, Phenanthrene, and Anthracene. *J. Phys. Chem.* **1996**, *100*, 15358–15367.

(117) Malloci, G.; Mulas, G.; Joblin, C. Electronic absorption spectra of PAHs up to vacuum UV, towards a detailed model of interstellar PAH photophysics. *Astron. Astrophys.* **2004**, *426*, 105–117.

(118) Hirata, S.; Lee, T. J.; Head-Gordon, M. Time-dependent density functional study on the electronic excitation energies of polycyclic aromatic hydrocarbon radical cations of naphthalene, anthracene, pyrene, and perylene. *J. Chem. Phys.* **1999**, *111*, 8904–8912.

(119) Christiansen, O.; Koch, H.; Jørgensen, P.; Helgaker, T. Integral direct calculation of CC2 excitation energies: singlet excited states of benzene. *Chem. Phys. Lett.* **1996**, *263*, 530–539.

(120) Matos, J. M. O.; Roos, B. O.; Malmqvist, P.-Å. A CASSCF-CCI study of the valence and lower excited states of the benzene molecule. *J. Chem. Phys.* **1987**, *86*, 1458–1466.

(121) Rubio, M.; Merchán, M.; Ortí, E.; Roos, B. O. A theoretical study of the electronic spectrum of naphthalene. *Chem. Phys.* **1994**, *179*, 395–409.

(122) Lorentzon, J.; Malmqvist, P.-Å.; Fülscher, M.; Roos, B. O. A CASPT2 study of the valence and lowest Rydberg electronic states of benzene and phenol. *Theo. Chim. Acta* **1995**, *91*, 91–108.

(123) Beck, M. E.; Rebentisch, R.; Hohlneicher, G.; Fülscher, M. P.; Serrano-Andrés, L.; Roos, B. O. Vertical and adiabatic electronic excitations in biphenylene: A theoretical study. *J. Chem. Phys.* **1997**, *107*, 9464–9474.

(124) González-Luque, R.; Serrano-Andrés, L.; Merchán, M.; Fülscher, M. P. Theoretical characterization of the absorption spectra of phenanthrene and its radical cation. *Theor. Chem. Acc.* **2003**, *110*, 224–232.

(125) Kawashima, Y.; Hashimoto, T.; Nakano, H.; Hirao, K. Theoretical study of the valence $\pi \rightarrow \pi^*$ excited states of polyacenes: anthracene and naphtacene. *Theor. Chem. Acc.* **1999**, *102*, 49–64.

(126) Marian, C. M.; Gilka, N. Performance of the density functional theory/multireference configuration interaction method on electronic excitation of extended π-systems. *J. Chem. Theory Comput.* **2008**, *4*, 1501–1515.

(127) *Dalton, a molecular electronic structure program*, release 2.0, 2005; http://www.kjemi.uio.no/software/dalton/dalton.html.

(128) Bendazzoli, G. L.; Evangelisti, S.; Palmieri, P.; Rettrup, S. A Configuration Interaction (CI) Procedure for the Evaluation of Two-Photon Electric Transition Probabilities. Program Implementation with Application to the $A_{1g} \rightarrow B_{2u}$ Transition of Benzene. *J. Chem. Phys.* **1986**, *85*, 2105–2111.

(129) Rettrup, S.; Bendazzoli, G. L.; Evangelisti, S.; Palmieri, P. A Symmetric Group Approach to the Calculation of Electronic Correlation Effects in Molecules. In *Understanding Molecular Properties*; Avery, J. S., Dahl, J. P., Hansen, A. E., Eds.; Reidel Publ. Co.: Dordrecht, Holland, 1987; pp 533−546.

(130) Guldberg, A.; Rettrup, S.; Bendazzoli, G. L.; Palmieri, P. A New Symmetric Group Programme for Direct Configuration Interaction Studies in Molecules. *Int. J. Quantum Chem., Quantum Chem. Symp.* **1987**, *21*, 513–521.

(131) Bendazzoli, G. L.; Palmieri, P.; Rettrup, S. A Permutation-group Direct Configuration Interaction Procedure for Second Order Molecular Properties. Program Implementation with Application to the $A^2\Sigma^+ \leftarrow X^2\Pi$ Two-Photon Transition of the OH Radical. *J. Chem. Phys.* **1989**, *91*, 5518–5527.

(132) Almost the experimental bond lengths since the reported experimental C−C bond length is 139.65 pm and the used bond length is 139.50 pm. The C−H bond length is 108.50 pm as experimentally measured.

(133) Stevens, R. M.; Switkes, E.; Laws, E. A.; Lipscomb, W. N. Self-consistent-field studies of the electronic structures of cyclopropane and benzene. *J. Am. Chem. Soc.* **1971**, *93*, 2603–2609.

(134) Pariser, R. Electronic Spectrum and Structure of Azulene. *J. Chem. Phys.* **1956**, *25*, 1112–1116.

(135) Hinchliffe, A.; Soscún, H. J. Ab initio studies of the dipole moment and polarizability of azulene in its ground and excited singlet states. *Chem. Phys. Lett.* **2005**, *412*, 365–368.

(136) Murakami, A.; Kobayashi, T.; Goldberg, A.; Nakamura, S. CASSCF and CASPT2 studies on the structures, transition energies, and dipole moments of ground and excited states for azulene. *J. Chem. Phys.* **2004**, *120*, 1245–1252.

(137) Chakrabarti, A.; Ramasesha, S. Properties of the low-lying electronic states of phenanthrene: Exact PPP results. *Int. J. Quantum Chem.* **1996**, *60*, 381–391.

(138) Rayez, J. C.; Dannenberg, J. J.; Kassab, E.; Evleth, E. M. A theoretical study of biphenylene in its ground and excited states. *J. Mol. Struct.* **1980**, *68*, 235–242.

(139) Elsaesser, T.; Lärmer, F.; Kaiser, W.; Dick, B.; Niemeyer, M.; Lüttke, W. Picosecond spectroscopy of electronically excited singlet states in biphenylene. *Chem. Phys.* **1988**, *126*, 405–416.

(140) Zimmermann, R. A theoretical study on the molecular structure of biphenylene in its first excited singlet and triplet states: quantum chemical calculations on the structural changes of an antiaromatic molecule upon excitation. *J. Mol. Struct.* **1996**, *377*, 35–46.

(141) Kautz, I.; Koch, T.; Malsch, K.; Hohlneicher, G. Ground state vibrations of biphenylene: experiment and theory. *J. Mol. Struct. (Theochem)* **1997**, *417*, 223–236.

(142) Hertzberg, J.; Nickel, B. Delayed $S_1 \rightarrow S_0$ and $S_2 \rightarrow S_0$ fluorescence, delayed excimer fluorescence, and phosphorescence from biphenylene. *Chem. Phys.* **1989**, *132*, 235–242.

(143) Fawcett, J. K.; Trotter, J. A refinement of the structure of biphenylene. *Acta Crystallogr.* **1966**, *20*, 87–93.

(144) Widmark, P.-O.; Malmquist, P.-Å.; Roos, B. O. Density matrix averaged atomic natural orbital (ANO) basis sets for correlated molecular wave functions I. First row atoms. *Theo. Chim. Acta* **1990**, *77*, 291–306.

(145) Mann, D. E.; Platt, J. R.; Klevens, H. B. Spectral Resemblances in Azulene and Naphthalene. *J. Chem. Phys.* **1949**, *17*, 481–484.

(146) Wilkinson, P. G. Absorption Spectra Of Benzene And Benzene-D6 In The Vacuum Ultraviolet. *Can. J. Phys.* **1956**, *34*, 596–615.

(147) Hochstrasser, R. M. The Absorption Spectrum of Diphenylene in the Near-Ultraviolet. *Can. J. Chem.* **1961**, *39*, 765–772.

(148) Inoue, H.; Hoshi, T.; Masamoto, T.; Shiraishi, J.; Tanizaki, Y. Dichroic Spectra of Anthracene, Acridine and Phenazine in Stretched PVA Sheets. *Ber. Bunsen-Ges. Phys. Chem.* **1971**, *75*, 441.

(149) Huebner, R. H.; Mielczarek, S. R.; Kuyatt, C. E. Electron energy-loss spectroscopy of naphthalene vapor. *Chem. Phys. Lett.* **1972**, *16*, 464–469.

(150) Bergman, A.; Jortner, J. Two-photon spectroscopy utilizing dye lasers. *Chem. Phys. Lett.* **1972**, *15*, 309–315.

(151) Bebelaar, D. Time resolved molecular spectroscopy using high power solid state lasers in pulse transmission mode. A re-examination of the $S_n \leftarrow S_1$ spectra of naphthalene and anthracene. *Chem. Phys.* **1974**, *3*, 205–216.

(152) Johnson, P. M. The multiphoton ionization spectrum of benzene. *J. Chem. Phys.* **1976**, *64*, 4143–4148.

(153) Dick, B.; Hohlneicher, G. Two-photon spectroscopy of the low-lying singlet states of naphthalene and acenaphthene. *Chem. Phys. Lett.* **1981**, *84*, 471–478.

(154) Fujii, M.; Ebata, T.; Mikami, N.; Ito, M. Electronic spectra of jet-cooled azulene. *Chem. Phys.* **1983**, *77*, 191–200.

(155) Johnson, P. M.; Korenowski, G. M. The discovery of a 3p Rydberg state in benzene by three-photon resonant multiphoton ionization spectroscopy. *Chem. Phys. Lett.* **1983**, *97*, 53–56.

(156) Dick, B.; Hohlneicher, G. Two-photon excitation spectroscopy of phenanthrene singlet states below 50000 cm $^{-1}$. *Chem. Phys. Lett.* **1983**, *97*, 324–330.

(157) Whetten, R. L.; Fu, K.-J.; Grant, E. R. Ultraviolet two-photon spectroscopy of benzene: A new gerade Rydberg series and evidence for the 1 $^1E_{2g}$ valence state. *J. Chem. Phys.* **1983**, *79*, 2626–2640.

(158) Grubb, S. G.; Otis, C. E.; Whetten, R. L.; Grant, E. R.; Albrecht, A. C. Higher excited states of benzene: Symmetry assignments of six gerade Rydberg series by four-photon absorption spectroscopy. *J. Chem. Phys.* **1985**, *82*, 1135–1146.

(159) Swiderek, P.; Michaud, M.; Hohlneicher, G.; Sanche, L. Electron-energy-loss spectroscopy of solid phenanthrene and biphenylene: Search for the low-lying triplet states. *Chem. Phys.* **1991**, *178*, 289–294.

(160) Hiraya, A.; Shobatake, K. Direct absorption spectra of jet-cooled benzene in 130−260 nm. *J. Chem. Phys.* **1991**, *94*-, 7700–7706.

(161) Rubio, M.; Manuela Merchán, M.; Ortí, E.; Roos, B. O. A theoretical study of the electronic spectrum of biphenyl. *Chem. Phys. Lett.* **1995**, *234*, 373–381.

(162) Foggi, P.; Neuwahl, F. V. R.; Moroni, L.; Salvi, P. R. $S_1 \rightarrow S_n$ and $S_2 \rightarrow S_n$ Absorption of Azulene: Femtosecond Transient Spectra and Excited State Calculations. *J. Phys. Chem. A* **2003**, *107*, 1689−–1696.

(163) Platt, J. R. Classification of Spectra of Cata-Condensed Hydrocarbons. *J. Chem. Phys.* **1949**, *17*, 484–495.

JP9037123